Localization and Activity of the Calcineurin Catalytic and Regulatory Subunit Complex at the Septum is Essential for Hyphal Elongation and Proper Septation in *Aspergillus fumigatus*

Praveen Rao Juvvadi[1], **Jarrod R. Fortwendel**[1,2], **Luise E. Rogg**[1], **Kimberlie A. Burns**[3], **Scott H. Randell**[3,4], and **William J. Steinbach**[1,2,*]

[1]Department of Pediatrics, Division of Pediatric Infectious Diseases, Duke University Medical Center, Durham, NC, USA

[2]Departments of Molecular Genetics and Microbiology, Duke University Medical Center, Durham, NC, USA

[3]Cystic Fibrosis/Pulmonary Research and Treatment Center, University of North Carolina, Chapel Hill, NC, USA

[4]Department of Cell and Molecular Physiology, University of North Carolina, Chapel Hill, NC, USA

Summary

Calcineurin, a heterodimer composed of the catalytic (CnaA) and regulatory (CnaB) subunits, plays key roles in growth, virulence, and stress responses of fungi. To investigate the contribution of CnaA and CnaB to hyphal growth and septation, Δ*cnaB* and Δ*cnaA* Δ*cnaB* strains of *A. fumigatus* were constructed. CnaA co-localizes to the contractile actin ring early during septation and remains at the center of the mature septum. While CnaB's septal localization is CnaA-dependent, CnaA's septal localization is CnaB-independent but CnaB is required for CnaA's function at the septum. Catalytic null mutations in CnaA caused stunted growth despite septal localization of the calcineurin complex, indicating the requirement of calcineurin activity at the septum. Compared to the Δ*cnaA* and Δ*cnaB* strains, the Δ*cnaA* Δ*cnaB* strain displayed more defective growth and aberrant septation. While three Ca^{2+}-binding motifs in CnaB were sufficient for its association with CnaA at the septum, the amino-terminal arginine-rich domains (16-RRRR-19 and 44-RLRKR-48) are dispensable for septal localization, yet required for complete functionality. Mutation of the 51-KLDK-54 motif in CnaB causes its mislocalization from the septum to the nucleus, suggesting it is a nuclear export signal sequence. These findings confirm a cooperative role for calcineurin complex in regulating hyphal growth and septation.

Keywords

Aspergillus fumigatus; calcineurin; cell wall; septum; hyphal growth; mutation

Introduction

Calcineurin, a Ca^{2+}/calmodulin (CaM)-dependent serine/threonine protein phosphatase type 2B, initially identified in muscle and brain (Stewart *et al.*, 1982), is ubiquitous and

---

[*]**Corresponding Author:** William J. Steinbach Department of Pediatrics Division of Pediatric Infectious Diseases Box 3499, Duke University Medical Center Durham, NC 27710 USA bill.steinbach@duke.edu Tel: (919) 681-1504 Fax (919) 668-4859.

conserved in all eukaryotes (Cyert, 2001, Sugiura *et al.*, 2002, Fox & Heitman, 2002). The core structure of calcineurin is composed of a heterodimer with a catalytic (CnaA; mol. wt ~60 kDa) and a regulatory (CnaB; mol. wt ~19 kDa) subunit. CnaA contains an amino-terminal catalytic domain that mediates interaction with phosphorylated substrates and a carboxy-terminal regulatory domain containing the CnaB binding helix (BBH), the CaM binding domain (CaMBD), and an autoinhibitory domain (AID) (Hemenway & Heitman, 1999, Aramburu *et al.*, 2000, Rusnak & Mertz, 2000). CnaB contains four EF hand Ca^{2+}-binding motifs and associates with CnaA. In the presence of Ca^{2+}, activated CaM binds to the CnaA-CnaB complex, resulting in a fully active trimeric phosphatase (Rusnak & Mertz, 2000). Among the three described protein serine/threonine phosphatases, calcineurin is the only phosphatase that requires Ca^{2+} and CaM for activity and exhibits restricted substrate specificity (Cohen & Cohen, 1989). The catalytic domain of calcineurin shows high sequence homology to the catalytic subunit of type 1 and 2A protein phosphatases, but differs in the presence of other C-terminal functional domains (Ito *et al.*, 1989).

In mammalian cells, three genes encoding the closely related isoforms of the catalytic subunit (CnAα, CnAβ, and CnAγ) and two genes encoding the regulatory subunit isoforms (CnB1 and CnB2) have been identified (Rusnak & Mertz, 2000). While CnAα and CnAβ isoforms are widely expressed, the CnAγ is expressed predominantly in the testes (Feske *et al.*, 2003). In accordance with these findings, CnB1 is ubiquitously distributed and binds to CnAα or CnAβ, but CnB2 is expressed in the testes and binds to CnAγ (Rusnak & Mertz, 2000). In addition to this differential distribution of the isoforms, variability in the molar ratio of CnA:CnB has also been reported, pointing to possible independent roles for each of the subunits in some tissues (Wei *et al.*, 1993, Li & Wei, 2001). In contrast to the calcineurin gene multiplicity observed in the mammals, lower eukaryotes such as the budding yeast *Saccharomyces cerevisiae* contain two genes encoding the catalytic subunit (*CNA1* and *CNA2*) and a single gene for the regulatory subunit (*CNB1*) (Cyert *et al.*, 1991). The fission yeast *Schizosaccharomyces pombe*, as well as filamentous fungal species, contain one gene encoding the catalytic subunit and one gene encoding the regulatory subunit of calcineurin (Yoshida *et al.*, 1994).

Calcineurin plays a central role in the regulation of cation homeostasis, morphogenesis, cell-wall integrity, stress and pathogenesis in fungi (Fox *et al.*, 2001, Fox & Heitman, 2002, Kraus & Heitman, 2003). Calcineurin is required for stress adaptation and pheromone-induced growth arrest in *S. cerevisiae* (Nakamura *et al.*, 1993, Moser *et al.*, 1996, Cyert, 2003, Kafadar & Cyert, 2004), and constitutive expression of a truncated catalytic subunit results in cell elongation with a unipolar budding pattern (Mendoza *et al.*, 1996). In the human pathogens *Candida albicans* and *Cryptococcus neoformans,* calcineurin regulates alkaline pH-mediated growth, membrane stress and virulence (Cruz *et al.*, 2002, Bader *et al.*, 2003, Reedy *et al.*, 2010, Chen *et al.*, 2010b). It is also required for mating and growth at elevated temperature in *C. neoformans* (Odom et al., 1997). Calcineurin participates in the morphogenesis of *S. pombe* by altering septal positioning and aberrant spindle body organization, and is implicated in membrane trafficking (Yoshida et al., 1994, Zhang *et al.*, 2000, Kita *et al.*, 2004). Previous reports in filamentous fungi have documented the importance of calcineurin for cell cycle progression in *Aspergillus nidulans* (Rasmussen *et al.*, 1994), hyphal branching in *Neurospora crassa* (Prokisch *et al.*, 1997), stress adaptation in *Aspergillus oryzae* (Juvvadi *et al.*, 2003), sclerotial development in *Sclerotinia sclerotiorum* (Harel *et al.*, 2006) and appressorium formation in *Magnaporthe oryzae* (Choi *et al.*, 2009). Earlier studies from our laboratory have shown that deletion of the catalytic subunit of calcineurin (*cnaA*) halts hyphal growth and virulence of *A. fumigatus* (Steinbach *et al.*, 2006). More recently, we also showed that CnaA localizes at the hyphal septum, suggesting a functional role for calcineurin in septum formation (Juvvadi *et al.*, 2008).

S. cerevisiae mutants lacking Cnb1p, or all three calcineurin subunits (Cna1p, Cna2p, and Cnb1p), are viable and *CNB1* mutants contain no detectable calcineurin activity, even in the presence of Cna1p and Cna2p, suggesting that the regulatory subunit is required for full enzymatic activity *in vitro* (Cyert & Thorner, 1992). Interestingly, the recombinant calcineurin catalytic subunit of *N. crassa* exhibits high activity even in the absence of its regulatory subunit (Higuchi *et al.*, 1991). In contrast to the filamentous fungal calcineurin, biochemical studies using a recombinant mammalian catalytic subunit suggested that the regulatory subunit as well as CaM is required for calcineurin activity (Perrino *et al.*, 1995). However, there have been no molecular genetic analyses evaluating the function of filamentous fungal calcineurin subunits *in vivo* and investigating if the catalytic subunit has functional activity in the absence of the regulatory subunit.

Filamentous fungi, with a single set of calcineurin catalytic and regulatory subunits, make ideal model systems to study the role of these subunits *in vivo*. Critically understanding the calcineurin pathway in *A. fumigatus* will also pave the way for devising new drug targets for combating invasive aspergillosis (Steinbach *et al.*, 2007b). To better understand how the calcineurin complex controls septum formation and hyphal growth, we simultaneously deleted both the catalytic and regulatory calcineurin subunits. In addition we mutated the regulatory subunit to identify regions essential for its localization and function with CnaA *in vivo*. Our results indicate that the calcineurin regulatory subunit is absolutely essential for activation of the catalytic subunit *in vivo*, and this complex selectively localizes at the septum to direct proper hyphal growth and regular septum formation.

Results

Construction and phenotypic analysis of the Δ*cnaB* and Δ*cnaA* Δ*cnaB* strains

Our previous work on the deletion of *cnaA* in *A. fumigatus* revealed its importance in both filamentous growth and virulence (Steinbach *et al.*, 2006). We also noted that CnaA concentrated as a disc around the septal pore in both newly formed and mature septa, revealing an invariably important role for calcineurin at the septum (Juvvadi *et al.*, 2008).

As an initial step towards understanding the relevance of the calcineurin catalytic and regulatory subunits for septation and hyphal growth in *A. fumigatus*, we performed a deletion analysis of the respective genes. The Af293-derived Af293.1 (uracil/uridine auxotroph) and Af293.6 (uracil/uridine and arginine auxotroph) isogenic strains (Xue *et al.*, 2004) were utilized to construct the single and double deletion strains, respectively. For construction of the double mutant, we first generated a Δ*cnaA* strain by replacement with the *A. fumigatus argB* marker gene in Af293.6 (Fig. 1). The resulting Δ*cnaA* strain was then transformed with the *cnaB* deletion allele harboring the *A. parasiticus pyrG* marker to replace the entire *cnaB* coding sequence to create a Δ*cnaA* Δ*cnaB* strain. Deletion of the respective genes was confirmed by Southern analysis (Fig.1A, B). The Δ*cnaA* and Δ*cnaB* strains were generated using the Af293.1 strain, and each single and double deletion strain was complemented (data not shown). All the deletion and complemented strains were analyzed for radial growth on GMM agar (Fig.1C). While all the complemented strains showed wild-type radial growth recovery, the Δ*cnaB* strain showed a compact colony morphology which was indistinguishable from the Δ*cnaA* strain (Fig.1C). In comparison to the single mutants, the Δ*cnaA* Δ*cnaB* strain showed slightly decreased radial growth. To more clearly define the subtle growth difference in the double mutant, different inocula sizes were spotted on GMM agar. As shown in Fig.1D, the Δ*cnaA* Δ*cnaB* strain grew slower than the single mutants, consistent with an additive growth defect caused by deletion of both calcineurin subunits.

Because a previous report (da Silva Ferreira *et al.*, 2007) suggested a role for calcineurin in inorganic phosphate utilization, we also examined the growth of the mutants on high dextrose/low phosphate SDA (Sabouraud dextrose agar) medium (Fig.1E). While growth of both the Δ*cnaA* and Δ*cnaB* strains diminished at lower inocula, the Δ*cnaB* strain showed slightly less growth than the Δ*cnaA* strain, which became more evident in the double mutant. Considering such phenotypes may be associated with cell wall defects or stress, we also tested if osmotic stabilizers could alleviate their growth defect. Interestingly, as shown in Fig.1F, only the growth of the Δ*cnaA* strain improved in the presence of sorbitol. In order to confirm if the partial sorbitol remediation occurred only in the *cnaA* deletion background we complemented the double mutant with *cnaA* or *cnaB* separately and found that only the double mutant complemented with *cnaB* showed similar improvement in growth in the presence of sorbitol (Fig.1F; see panel Δ*cnaA* Δ*cnaB* + *cnaB*). Hyphal growth recovery of the double mutant complemented with either *cnaA* or *cnaB* was also monitored in GMM liquid medium after 24 h and as shown in Suppl. Fig.S1, whereas the Δ*cnaA* Δ*cnaB* double mutant grew much slower, the Δ*cnaA* Δ*cnaB*+*cnaA* and Δ*cnaA* Δ*cnaB*+*cnaB* strains exhibited similar growth as the individual single mutants (Δ*cnaA* or Δ*cnaB*).

Calcineurin double mutant exhibits delayed germination, irregular branching, and aberrant septum formation

Because the Δ*cnaA* Δ*cnaB* strain grew slower than the single mutants, we also monitored the rates of germination in the mutant strains. As shown in Fig. 2A, while both the single mutants (Δ*cnaA* and Δ*cnaB*) and the double mutant complemented with either CnaA or CnaB (Δ*cnaA* Δ*cnaB*+*cnaA*; Δ*cnaA* Δ*cnaB*+*cnaB*) displayed germination rates comparable to the wild-type, the Δ*cnaA* Δ*cnaB* strain exhibited a lag in germination. In comparison to the single mutants or the double mutant complements, in which the germination rate was 100% at the end of 7 hours, the Δ*cnaA* Δ*cnaB* strain had a germination rate of only 87% after 13 hours. It is likely that some conidia were not viable as we did not observe completion of germination beyond 14 hours. Light microscopy of the strains showed more stunted and irregularly branched hyphae in the Δ*cnaA* Δ*cnaB* strain at 18 hours of growth (Fig. 2B). The hyphal compartments in the double mutant also seemed slightly swollen with abnormal septation compared to the single mutants. To further quantify the hyphal growth and irregular septation defects in the single (Δ*cnaA* and Δ*cnaB*) and double (Δ*cnaA* Δ*cnaB*) mutants, the strains were grown for a period of 24 and 48 h hours, respectively, and the length of the various hyphal compartments (apical, sub-apical and basal) were measured. As shown in Fig. 4D, all the calcineurin deletion strains showed shorter hyphal compartments. In comparison to the wild-type strain, while the apical compartment and the second compartment (sub-apical) lengths in the single deletion strains were reduced by approximately 50%, there was almost 70% reduction in size of both these compartments in the double mutant. The older basal compartments also showed an 80% reduction in size in the double mutant, revealing that septation occurred more irregularly in the double mutant.

Scanning electron microscopy (SEM) was performed to delineate changes in the hyphal architecture between the calcineurin mutants. Unlike the wild-type strain which contained fully-extended hyphae with normal morphology, the Δ*cnaA* strain grew as a compact colony and had blunt hyphae with irregular branching at the tips (Fig. 2C). In contrast to the blunted club-like appearance of hyphae in the Δ*cnaA* strain, both the Δ*cnaB* and the Δ*cnaA* Δ*cnaB* strains formed straighter hyphae (Fig. 2C). Interestingly, whereas all the mutant strains showed a mesh-like fibrous material (indicated by white arrows) that seemed to adhere the hyphae together, the fibrous layer was more prominent in the Δ*cnaB* and the Δ*cnaA* Δ*cnaB* strains (Fig. 2C). SEM of each of the complemented strains (Δ*cnaA*::*cnaA*; Δ*cnaB*::*cnaB*; Δ*cnaA* Δ*cnaB*::*cnaA cnaB*) showed normal hyphal morphology without any webbing (data not shown). Although the nature of this extracellular fibrous material is unknown, it may be

a mixture of polysaccharides and mannoproteins that are improperly assembled due to defects in cell wall synthesis resulting from the deletion of the calcineurin genes.

To further explore the requirement of the functional calcineurin complex for proper cell wall architecture, we examined the morphology of the cell wall by transmission electron microscopy (TEM). While the cell wall of the wild-type strain appeared as a uniform layered structure exhibiting an electron-dense layer (Fig. 3; panels B and C), each of the calcineurin mutants displayed aberrant cell wall architecture. The cell wall was thicker in all of the deletion mutants in comparison to the wild type (Fig. 3; panels D-O). The inner layer, which mostly consists of glucan, seemed enlarged, and the outer layer, which contains mannoproteins, was thicker (indicated by dotted arrows). While both the Δ*cnaA* and Δ*cnaB* strains showed abnormal septa (Fig. 3; panels D-I; indicated by arrowheads), the Δ*cnaA* Δ*cnaB* strain had curved and often wavy and incomplete septa (Fig. 3; panels J-O; indicated by arrowheads). On closer inspection of some of the hyphal compartments, septum formation in the Δ*cnaA* Δ*cnaB* strain was not coordinated properly from both sides of the hyphal wall, resulting in incomplete septum formation (Fig. 3; panels L and N). The observed septation defects in the three calcineurin deletion strains were quantified by counting the septa (>200 septa in each strain) after calcofluor white staining. In comparison to the Δ*cnaA* and Δ*cnaB* strains, which showed an average of 56% and 60% of abnormal septa, respectively, the Δ*cnaA* Δ*cnaB* strain showed 70% of abnormal septa. Although sorbitol partially remediated the growth defect of Δ*cnaA* strain, it did not restore normal hyphal septation (data not shown). The calcineurin complex may therefore be important for the correct deposition of new cell wall material at the septum and for normal cell wall structure. Collectively, these results indicated that the calcineurin mutants may have an inherent defect in the composition of their cell walls.

Calcineurin A and B coordinately function for proper cell wall organization

Since the Δ*cnaA* Δ*cnaB* strain exhibited increased cell wall and septation defects, we sought to explain these phenotypes by performing calcoflour white and aniline blue staining of the mutants to look for any alterations in the distribution of the two major cell wall components, chitin and β-glucan. As shown in Fig. 4A, although no significant differences could be noted in the distribution of chitin at the septa in the respective mutants, the Δ*cnaA* Δ*cnaB* strain showed wavy and incomplete septa (Fig. 4A; 4B; indicated by arrows), confirming the TEM observation (Fig. 3). Previous reports on the characterization of the chitin synthase double mutant (Δ*chsA* Δ*chsC*) and a Δ*chsB* single mutant in *Aspergillus nidulans* also showed irregular septation and wavy/incomplete septa (Ichinomiya *et al.*, 2005, Fukuda *et al.*, 2009).

Because the septa of the double mutant were incomplete and abnormal, we next stained with propidium iodide to examine nuclear distribution. Some compartments were devoid of any nuclei and nuclei could be seen passing through the incomplete septa of the double mutant (Fig. 4B; septa indicated by arrows), a phenomenon not observed in the wild type or single deletion strains (data not shown). Deletion of *cnaA* has previously been shown to decrease nuclear division kinetics (da Silva Ferreira et al., 2007). Aniline blue (0.1%), which stains cell wall β-glucan, did not show septal staining in the Δ*cnaA* Δ*cnaB* strain after a 24 h growth period (Fig. 4C; panel for Δ*cnaA* Δ*cnaB*; indicated by arrows). To clarify if the double mutant had no β-glucan deposition at all or less β-glucan at 24 h growth period, we utilized a higher concentration of aniline blue (0.5%) but could not detect septal staining. However, we could detect β-glucan staining at the septa of the Δ*cnaA* Δ*cnaB* strain after a 48 h growth period, which indicated that there is a lag in the assembly of septal wall material in the double deletion strain. It is possible that the double mutant has less β-glucan deposition at the septum during early phase of growth. These results indicate that, in comparison to the single deletion strains, deletion of both the subunits of calcineurin is more deleterious and results in greater abnormality of the cell wall and septa.

The growth defect and septation abnormality in the double mutant indicated either a lack of proper synthesis of the major cell wall components, chitin and β-glucan, or an improper assembly of these components. We therefore next assayed for the total β-glucan and chitin contents of the strains. The β-glucan content in all the calcineurin mutants was reduced by ~40% when compared to the wild-type strain (Fig. 5A). This reduction in the β-glucan content of the Δ*cnaA* strain correlates with our previous report (Cramer *et al.*, 2008). In contrast to the decreased β-glucan content of the calcineurin mutants, an increase in the chitin levels was noted in all the mutants, with the Δ*cnaA* Δ*cnaB* strain showing an increase of ~40% and each Δ*cnaA* and Δ*cnaB* strain showing ~20% increase when compared to the wild-type strain (Fig. 5B). We have earlier reported such compensatory increases in the chitin contents of strains treated with caspofungin, an inhibitor of β-1,3-glucan synthase (Fortwendel *et al.*, 2009). Although we observed an increased growth defect in the Δ*cnaA* Δ*cnaB* strain when compared to the single mutants, there were no statistically significant variations in both the major cell wall components when comparing the single and double mutants. To investigate if exogenous β-glucan could ameliorate the growth defect of the calcineurin mutants, β-1,3-glucan in the form of curdlan (Sigma) was supplemented at a concentration range of 0.01-0.1% in GMM medium, but we did not observe any improvement in the growth of all the mutants (data not shown).

Although we did not visualize any significant differences among the mutants in staining with calcoflour white in comparison to the wild-type, there was a statistically significant increase in chitin content of the mutants (Fig. 5B). As this may be a cell wall stress compensatory mechanism due to the deletion of the calcineurin subunits, we analyzed the transcriptional profile of all the chitin synthase genes in the mutants. Interestingly, analysis of the transcriptional profiles of eight chitin synthase genes (*chsA, chsB, chsC, chsD, chsE, chsF, chsG* and *chsEb*) in the Δ*cnaB* and Δ*cnaA* Δ*cnaB* strains showed a downregulation of all the chitin synthase genes (data not shown) as was previously reported in the Δ*cnaA* strain (Cramer et al., 2008). The abnormality in the assembly of the cell wall components in the calcineurin mutants may result from the impaired incorporation of chitin in the cell wall due to the decreased proportion of β-glucan. Previous results from our laboratory have indicated an ~2-fold decrease in the transcription of *fksA*, encoding the catalytic subunit of β-1,3-glucan synthase, in the Δ*cnaA* strain (Cramer et al., 2008), which coincides with our present observation of decreased β-glucan levels in all the calcineurin mutants.

Calcineurin complex localizes to the site of septation early during septum formation

We previously showed that apart from localizing at the septa, CnaA concentrates as punctate dot-like structures at the hyphal tips and in developing conidiophores (Juvvadi *et al.*, 2008). Since the Δ*cnaB* strain showed a similar growth phenotype as deletion of *cnaA* (Steinbach et al., 2006), indicating a cooperative regulation between the catalytic and regulatory subunits, we were interested in analyzing the localization patterns of both CnaA and CnaB. The Δ*cnaA* Δ*cnaB* strain was co-transformed with *cnaA-egfp* and *mcherry-cnaB* fusion constructs (under the control of their respective native promoters) and the complemented strain obtained showed complete restoration of hyphal growth (Fig. 1), demonstrating functionality of the fusion proteins. Fluorescence microscopy of the complemented strain showed the co-localization of mcherry-CnaB and CnaA-EGFP at the septa (Fig. 6A). Time lapse microscopy of the calcineurin complex revealed that the dot-like structures initially present in the swollen conidium concentrated at the point of germ tube emergence and remained at the tip of the germling as hyphal extension occurred (Fig. 6B; Supplementary movie 1). The punctate structures moved from the hyphal tip towards the septation initiation sites and then concentrated at the center of the septum soon after the septum formation (Supplementary movie. 2).

In order to more clearly analyze the septal localization of CnaA relative to the actin ring, we transformed the OCNAG3 strain expressing CnaA-EGFP with a Lifeact-RFP vector and visualized both CnaA and actin network during growth and septation. We found that CnaA-GFP punctate spots co-localized with the Lifeact-RFP which decorated the contractile ring that formed at the initial stages of actin ring formation at the place of new septum (Fig. 7A-F). The CnaA-GFP remained at the septa even after the actin ring diffused from the completely formed septum (Fig. 7G; completely formed septum indicated by dashed circle). This indicated that the calcineurin complex appears early in the process of septation and is present throughout the process of septum formation. The presence of calcineurin during the initial germination phase and then during hyphal extension and septation indicated a diverse role for calcineurin in morphogenetic control. Because we found that calcineurin co-localized with the contractile actin ring at the sites of septation, we were interested to verify if the septation defects caused in the Δ*cnaA* Δ*cnaB* strain were due to defects in actin organization. To test this we expressed the Lifeact-RFP in the wild-type and the calcineurin double mutant background and compared the formation of the actin rings. The Δ*cnaA* Δ*cnaB* strain showed normal actin ring formation as was observed with the wild-type strain (Suppl. Fig. S2), indicating that the calcineurin complex may not be involved in actin organization during early septation process but may control the activation of cell wall biosynthetic components at the septum during primary or secondary stages of septum formation.

Catalytic activity of calcineurin A is not required for localization of the calcineurin complex at the septum

Previous studies in mammalian cells have shown that both CnA and CnB are required for binding by the immunophilin-immunosuppressant complexes (FKBP12-FK506 and cyclophilin-CsA) (Clipstone *et al.*, 1994). FKBP acts as a "scaffold" protein to localize calcineurin to its site of action, and the localization of FKBP12 and calcineurin to the ryanodine receptor can be disrupted by adding FK506 (Cameron *et al.*, 1995). As the immunophilin-immunosuppressant complex binds to the CnaA-CnaB complex, we examined the effect of FK506, an inhibitor of calcineurin activity, on localization of the calcineurin complex at the septum. Treatment with FK506 or cyclosporin A did not affect localization of the calcineurin complex at the septum, although the treatment resulted in a phenotype that resembled a calcineurin deletion (data not shown). This result indicated that calcineurin activity is not required for localization of the calcineurin complex at the septum. In order to verify if calcineurin activity is essential for septal localization, we next constructed catalytic null mutations in CnaA. Three residues (Ser[373], His[375] and Leu[379]) that lie in the linker region between the catalytic domain and the CnaB binding helix of CnaA (Fig. 8A) have previously been shown to be crucial for catalytic activity in *S. cerevisiae*, but at the same time these mutations did not affect the binding to CnaB, calmodulin or Fkbp1(Jiang & Cyert, 1999). As shown in the amino acid sequence alignment with *S. cerevisiae* CNA1 and Human CNAα, this region is highly conserved, except for Thr[359] in place of Ser[373] in the *A. fumigatus* CnaA (Fig. 8A). We mutated the two residues Thr[359] and Leu[365] to Pro[359] (T359P) and Ser[365] (L365S), respectively. Expression of both the CnaA catalytic null mutations (CnaA-T359P; CnaA-L365S) along with mcherry-CnaB under the control of their native promoters in the Δ*cnaA* Δ*cnaB* strain did not affect the localization of the calcineurin complex (CnaA-T359P-GFP and mcherry-CnaB; CnaA-L365S-GFP and mcherry-CnaB) at the septa as shown in Fig. 8 B-C, but the growth of the respective strains was drastically affected (Fig. 8D). Assay for calcineurin enzymatic activity using *p*-nitrophenyl phosphate as a substrate in these strains also revealed a dramatic reduction in the activity (~70-80%) in comparison to the wild-type strain, indicating that these mutations affected the catalytic function of CnaA (Fig. 8E). Though the catalytic null mutant strains grew a little better than the Δ*cnaA* Δ*cnaB* strain, they remained stunted. This

indicated that although the calcineurin complex localizes at the septum, calcineurin activity is absolutely essential at the septum to direct proper septation and hyphal growth. Furthermore we also noted that sorbitol partially remediated the growth defect in the catalytic null mutants (Fig. 8D), similar to the observations made with the Δ*cnaA* strain or the Δ*cnaA* Δ*cnaB*+cnaB strain (Fig. 1F).

Localization of calcineurin B at the septum requires complex formation with calcineurin A

Next, to define if each individual subunit can independently localize at the hyphal septum, we localized CnaB in the Δ*cnaA* deletion background and CnaA in the Δ*cnaB* deletion background. As shown in Fig. 9A, CnaB remained in dot-like structures which were evenly distributed in the hyphal compartments, without septal-localization in the absence of CnaA. However, CnaA localized to the hyphal septum even in the absence of CnaB (Fig. 9B). Although CnaA localizes at the septa independent of CnaB, the Δ*cnaB* phenotype could not be restored to that of the wild-type strain, indicating the absolute requirement of CnaA complexing with CnaB for normal calcineurin function and activity at the hyphal septum. Furthermore, this unexpected result indicated that CnaA may localize at the septum by binding to other as yet undefined proteins. To verify if CnaA alone has catalytic activity in the absence of the CnaB regulatory subunit we assayed for calcineurin phosphatase activity. As shown in Fig. 8E, in comparison to the wild-type strain, the Δ*cnaB* strain showed ~80% reduction in calcineurin activity, indicating the requirement of the regulatory subunit for its activation. In our assays the Δ*cnaA* and the Δ*cnaA* Δ*cnaB* strains showed similar reduction values (~90%) for the amounts of *p*-nitrophenyl phosphate hydrolyzed. Based on these results it is possible that the remaining amount *p*-nitrophenol released is non-specific to calcineurin.

Ca^{2+}-binding sites I, II and III in calcineurin B are sufficient for localizing at the hyphal septum with calcineurin A

Calcineurin B contains four EF hand type Ca^{2+}-binding motifs (Kretsinger, 1980) (Fig. 8A). While inactivation of the first three Ca^{2+}-binding sites reduces phosphatase activity (Kakalis *et al.*, 1995), truncated Ca^{2+}-binding domains (Fig. 10A; Domain 1 and Domain 2) with only two Ca^{2+}-binding sites can still bind to calcineurin A and stimulate its activity in the presence of calmodulin *in vitro* (Jiang & Wei, 2003). Ca^{2+}-free calcineurin B has also been shown to bind to calcineurin A and regulate its activity, albeit to a lesser extent than Ca^{2+}-saturated calcineurin B (Li & Wei, 2001). Although we showed that CnaA localized at the septa independent of CnaB, the fact that CnaB is required for functionality prompted us to examine if truncated forms of CnaB can still bind to CnaA *in vivo* and localize at the hyphal septum. We constructed several truncated forms of CnaB (Fig. 10A), and individually expressed them in the wild-type background. Based on the localization pattern obtained, we could classify each truncated strain into one of the two categories of either septal or cytosolic CnaB localization. We found that just the first 3 Ca^{2+}-binding sites were sufficient for CnaB to localize at the septum (construct tB-3). Expression of constructs missing the extended N-terminal portion preceding the first Ca^{2+}-binding site also showed septal localization (tB-1 and tB-2), indicating that this part of the protein may not be necessary for binding to CnaA and localizing at the septum. The other truncations, including those containing domain 1 and domain 2, showed cytosolic localization. Our *in vivo* findings somewhat support the previous report indicating that inactivation of first 3 Ca^{2+}-binding sites reduces calcineurin activity *in vitro* (Kakalis et al., 1995), but we did not observe septal localization of the individual domain 1 and domain 2 constructs (tB-7 and tB-8). It is possible that these truncated constructs do not interact with CnaA *in vivo* and therefore do not localize at the septum. To more clearly correlate the requirement for CnaB's localization at the septum for function and also to rule out the possibility of mislocalization of the truncated CnaB fragments due to the overexpression from the *otef* promoter in the wild-type

background, we also expressed the various constructs under the control of the CnaB native promoter in the Δ*cnaB* strain and verified for complementation and septal localization. As shown in Fig. 10B, none of the CnaB truncated constructs complemented the Δ*cnaB* mutant phenotype and all the truncations examined mislocalized to the cytosol, confirming our previous observation on their localization pattern in the wild-type background.

N-terminal and C-terminal regions are dispensable for calcineurin B localization at the septum but essential for complete functionality

We found that the first 3 Ca^{2+}-binding sites were sufficient for localization of CnaB at the septum, thus we wanted to further clarify to what extent these truncated forms of CnaB can interact with and activate CnaA at the hyphal septum for restoration of hyphal growth. For this we used the truncation, CnaB-tB3, which lacks the 4th Ca^{2+}-binding site, and a domain swapped construct, CnaB-SW2, made by swapping the extended stretch of the N-terminal CnaB region with the shorter N-terminal region of its human counterpart, CnB1 (Fig. 11A). We chose to use the CnaB-SW2 construct because a comparative analysis of the amino acid sequence of *A. fumigatus* CnaB with human CnB1 revealed an extended stretch of the N-terminal region consisting of an arginine-rich cluster (15-ARRRRA-20) in *A. fumigatus* CnaB (Fig. 11A) not seen in human CnB. The entire N-terminal stretch of residues 1-43 were substituted for the human CnB1 residues 1-21, creating a cnaB-SW2 construct which was then transformed into the Δ*cnaB* strain and verified for complementation. Each of the constructs expressed in the Δ*cnaB* strain localized at the hyphal septum and restored hyphal growth, but not to the extent of full length CnaB (Fig. 11B and C). This indicated that fungal-specific residues in the N-terminal and C-terminal regions of CnaB are required for complete functionality of the calcineurin complex.

As the extended stretch of basic amino acid residues in the N-terminal region (15-ARRRRA-20) of *A. fumigatus* CnaB is unique to filamentous fungi, it is possible that these residues might serve as a binding site for a motif with opposite charge and identical hydrophobicity. Therefore, we wanted to further investigate if this region is essential for function and localization of calcineurin complex at the septa. We mutated all the arginines to glycines (Fig. 12B; panel CnaB^RRRR-GGGG) and transformed the CnaB mutated construct into the Δ*cnaB* strain. As shown in Fig. 12B, the CnaB^RRRR-GGGG –GFP fusion protein did not mislocalize from the septa. Although hyphal growth of the CnaB^RRRR-GGGG strain was restored and resembled wild type growth at the end of 3 days, a radial growth reduction of ~25% was noted at the end of 5 days of growth. Expression of the CnaB^RRRR-GGGG-GFP fusion construct was verified by Western analysis (Fig.12E; See lane corresponding to CnaB^RRRR-GGGG). This indicated that, although the unique stretch of arginines at the N-terminus is not essential for binding to CnaA and localizing at the septum, it may be required for binding to other unknown effectors or for complete functionality of CnaA at the septum.

Mutation causing mislocalization of calcineurin B from the septa reveals the absolute requirement of the calcineurin complex for hyphal growth

The N-terminal residues 15-FDADEIKRLGKRFKK-29 in mammalian calcineurin B form an amphiphilic helix (West *et al.*, 1993), and mutations within this cluster of basic residues results in the inability of calcineurin to bind to phosphatidylserine vesicles but has no effect on N-terminal myristoylation, Ca^{2+}-binding, or calcineurin heterodimer formation and phosphatase activity *in vitro* (Martin *et al.*, 2001). Closer examination of the residues in the sequence overlapping this region revealed a potential nuclear export signal sequence (NES) with a consensus motif LxxxLxxLxL (22-RLGKRFKKLDLDNSGSL-38; conserved residues are underlined; Fig. 12A). Moreover, analysis of this sequence using the NetNES 1.1 program (la Cour *et al.*, 2004) also predicted it as a potential NES sequence. Leucine-

rich NES signals usually consist of 4-5 hydrophobic residues within a region of ~10 amino acids that are predominantly leucine, but may also be isoleucine, valine, methionine and phenylalanine. As this sequence is also conserved in *A. fumigatus* CnaB at position 44-RLRKRFMKLDKD-55, we were interested in determining if mutations in this region would complement the Δ*cnaB* phenotype and localize CnaB at the hyphal septum *in vivo*. We performed site-directed mutagenesis of the 44-RLRKR-48 residues to 44-AAAAA-48, and 51-KLDK-54 to 51-AAAA-54, respectively. The CnaB mutated constructs were then individually transformed into the Δ*cnaB* strain to assess localization pattern and complementation. As shown in Fig. 12B (see panel CnaB$^{RLRKR-AAAAA}$), the strain harboring the RLRKR-AAAAA mutation exhibited fairly normal hyphal growth, although there was a decrease in growth rate compared to the control strain (Fig. 12C). Moreover, the localization of CnaB$^{RLRKR-AAAAA}$-GFP fusion protein was clearly seen at the hyphal septum (Fig. 12B; see panel CnaB$^{RLRKR-AAAAA}$). Expression of the CnaB$^{RLRKR-AAAAA}$-GFP fusion construct was verified by Western analysis (Fig. 12E; See lane corresponding to CnaB$^{RLRKR-AAAAA}$). As the RLRKR-AAAAA mutation complemented the Δ*cnaB* strain and did not have any effect on the localization of CnaB at the septum, it is clear that this region is not involved in binding of CnaB to CnaA *in vivo* as was shown earlier by *in vitro* studies (Martin et al., 2001). In contrast, the KLDK-AAAA mutation mislocalized the CnaB-GFP fusion protein to the nucleus and only partially complemented the mutant phenotype (Fig. 12B). This partial complementation however did not restore normal septation or changes in the length of the hyphal compartments, indicating that CnaB function at the hyphal septum is important for regulating normal hyphal extension and septation (data not shown). Expression of the CnaB$^{KLDK-AAAA}$-GFP fusion construct was also verified by Western analysis (Fig. 12E; See lane corresponding to CnaB$^{KLDK-AAAA}$). Although *A. fumigatus* CnaB does not show conservation in the 4th leucine residue when compared to mammalian calcineurin B, it is interesting to note that other residues such as aspartic acid are usually favored at the C-terminus in the NES region. As shown in Fig. 12A, *A. fumigatus* CnaB has two aspartic acid residues close to the leucine residue. Earlier studies have indicated that leucines in the C-terminal end of the NES are more important for function (Wen *et al.*, 1995), thus it is possible that the entire 44-RLRKRFMKLDKD-55 region is the actual NES of *A. fumigatus* CnaB. Although we have not observed the localization of calcineurin complex in the nucleus, taken together these results indicate that the calcineurin complex does localize transiently to the nucleus, but accumulation of the regulatory subunit within the nucleus due to the mutation in the identified NES leads to the growth defect as a result of lack of interaction of CnaA and CnaB at the hyphal septum.

Discussion

In addition to the established role of calcineurin in the stress response pathways of yeasts and filamentous fungi (Bonilla *et al.*, 2002, Cyert, 2003, Juvvadi et al., 2003, Kraus & Heitman, 2003, Lagorce *et al.*, 2003, Heath *et al.*, 2004, Bader *et al.*, 2006), its role in mediating the septation initiation network has previously been shown in *S. pombe* (Zhang et al., 2000, Yada *et al.*, 2001, Lu *et al.*, 2002) and *C. neoformans* (Fox *et al.*, 2003) through coordinated regulation of other proteins. However, not much is known of its role in septum formation in filamentous fungi. Recent results from our laboratory have more precisely shown that the catalytic subunit of calcineurin in *A. fumigatus* localizes at the hyphal septum (Juvvadi et al., 2008) and its deletion causes stunted hyphal growth, irregular septation and the phenotype mimics the pharmacologic inhibition of calcineurin by FK506 and cyclosporin A (Steinbach et al., 2006).

Here we report some differing phenotypic effects resulting from deletion of individual subunits of calcineurin (*cnaA* and *cnaB*) and the complex as a whole, suggesting a previously unsuspected complexity in their individual functions. The Δ*cnaA* and Δ*cnaB*

strains exhibited a similar germination pattern, whereas the Δ*cnaA* Δ*cnaB* strain showed a lag in germination. Only the growth of the strains lacking functional CnaA were partially remediated by sorbitol, indicating the possibility of differences in the cell wall components of the individual Δ*cnaA* and Δ*cnaB* mutants or an osmotic defect in the Δ*cnaA* strain. Involvement of calcineurin in osmotic stress response pathways through the PKC and HOG pathways has previously been reported in yeasts and filamentous fungi (Garrett-Engele *et al.*, 1995, Delgado-Jarana *et al.*, 2006). Although the content of the major cell wall constituents, β-glucan and chitin, did not reveal any specific variations between the single and double mutants, only the Δ*cnaA* Δ*cnaB* strain septa were not stained by aniline blue at 24 h growth period, which normally binds β-glucan. Moreover, the Δ*cnaA* Δ*cnaB* strain showed a higher percentage of abnormal wavy septa that were incomplete and disorganized. Although we did note the presence of β-glucan at the septum at 48 h growth period in the Δ*cnaA* Δ*cnaB* strain, it is possible that the arrangement of β-glucan at the septum might be affected by simultaneous deletion of both calcineurin subunits. Extracellular web-like material observed in the Δ*cnaB* and Δ*cnaA* Δ*cnaB* strains further suggests the possibility of highly disordered cell wall architecture in these mutants. These differences might be contributing to its somewhat more severe growth phenotype in comparison to the individual single deletion mutants.

Dynamic movement of the calcineurin complex in punctate structures during initial germ tube emergence and then subsequent concentration at the hyphal tip and throughout the process of septum formation indicated its role at active points of growth and septation. Moreover, co-localization of the CnaA-GFP puncta with the actin ring during the early stages of septation also indicated its role in both primary and secondary events of septum formation. In contrast to the transient localization of proteins that are known to play vital role in cell wall integrity pathways, e.g., protein kinase C, protein phosphatase 1 (BimG) and calmodulin, at the septum (Fox *et al.*, 2002, Teepe *et al.*, 2007, Chen *et al.*, 2010a), the calcineurin complex remains at the hyphal septum even after actin dissipates, indicative of a major role for this phosphatase in the formation and maintenance of septum.

While activity studies on calcineurin from mammalian cells have indicated a requirement for the regulatory subunit as well as CaM for the activation of calcineurin A (Merat *et al.*, 1985), reports on the calcineurin A-independent existence of calcineurin B have also suggested exclusive functions for the regulatory subunit (Wang *et al.*, 2008). Point mutations or truncations in calcineurin B have provided evidence of the importance of the regulatory subunit for activation of calcineurin A (Jiang & Wei, 2003, Li *et al.*, 2009). Intriguingly, recombinant *N. crassa* calcineurin catalytic subunit exhibited high activity in the absence of its regulatory subunit, revealing that the Ca^{2+}-binding subunit is not a prerequisite for its activation (Higuchi et al., 1991).

Although there has been one report on the deletion of calcineurin B in *N. crassa* (Kothe & Free, 1998), functional analysis of the individual subunits and residues required for their function *in vivo* in filamentous fungi has never been investigated. To more clearly understand the cooperative role for the calcineurin subunits *in vivo* and verify if the catalytic subunit has functional activity in the absence of the regulatory subunit, we localized each of the subunits in the absence of the other and monitored for recovery of hyphal growth. In the absence of CnaA, CnaB was completely mislocalized, but unexpectedly, CnaA still localized to the hyphal septum in the absence of CnaB. However, localization of CnaA alone at the septum did not complement the mutant phenotype, revealing that CnaB is absolutely required for the full activation of the calcineurin complex *in vivo*. Drastic reduction of calcineurin activity in the Δ*cnaB* strain further supported the requirement of the regulatory subunit for functional activity of CnaA. Moreover, catalytic null mutations in CnaA revealed the requirement for both localization and activity of the calcineurin complex at the hyphal

septum. To verify the important domains in CnaB that are required to complex with CnaA, we expressed truncated forms of CnaB labeled with GFP and confirmed that only three of the four Ca^{2+}-binding domains in CnaB are sufficient for septal targeting of the calcineurin complex. The C-terminal region, though not required for binding to CnaA and septal targeting, is necessary for complete functionality of the complex *in vivo*. Furthermore, the requirement for localization of CnaB at the septum to direct proper hyphal growth and septation was confirmed by complementation of the truncated forms of CnaB in the Δ*cnaB* strain.

While the human CnB1 and *A. fumigatus* CnaB are highly conserved, there is one region of striking divergence between these proteins. The amino terminus of *A. fumigatus* CnaB is extended and contains a unique arginine-rich sequence in addition to a conserved polybasic domain that is also present in human CnB1. Since a string of basic residues at the amino terminus may contribute significantly to protein localization (Sigal *et al.*, 1994), we speculated that such motifs might contribute to substrate-specific protein-protein interactions or have a role in the binding of the calcineurin complex to the septa. While mutations in the 15-ARRRRA-20 and 44-RLRKR-48 motifs showed that CnaB is predominantly in the cytoplasm and concentrated at the septa as a complex with CnaA, mutation in the potential NES sequence (51-KLDK-54) resulted in its accumulation in the nucleus and a phenotype that resembled the Δ*cnaB* strain. How CnaB nuclear and cytoplasmic localization is regulated, and if each has distinct functions, remains unknown. Previous reports have shown the co-migration of calcineurin and NFAT into the nucleus, and that calcineurin is required to maintain NFAT in a dephosphorylated state for sustained activation of its targets (Zhu & McKeon, 1999). Although it is well established that the dephosphorylation of Crz1p by calcineurin leads to its nuclear translocation (Stathopoulos-Gerontides *et al.*, 1999), there are no reports of the nuclear localization of calcineurin B in the yeasts or filamentous fungi. Nuclear localization of a calcineurin B homologous protein (CHP1) has been reported (Nagita *et al.*, 2003, Jiménez-Vidal *et al.*, 2010). We could not identify any potential NLS sequence in the *A. fumigatus* CnaB and it is possible that CnaB may translocate into the nucleus with CnaA and CrzA. Under normal conditions we were not able to detect nuclear localization of either CnaA or CnaB subunits. It is possible that their concentration in the nucleus is below detectable limits or the localization is very transient. It is also possible that CnaB has spatially distinct functions, as we observed CnaB in punctate structures and in the cytosol under normal conditions. An optimal balance in the ratio of CnaA to CnaB is important in various cellular compartments, as we see that an accumulation of CnaB in the nucleus due to mutation of the NES does not support normal hyphal growth.

It has been noted that in some tissues the molar ratio of CnA to CnB is not equal, and sometimes more CnB than CnA or even only CnB exists (Wang et al., 2008). Excess expression of *CNB* in the absence of *CNA* has been shown in mitochondria, and other studies have also shown that there is excess CnB in comparison to CnA in the brain (Li & Handschumacher, 2002). Moreover, CnB promoted the expression of TNF-α/CHX-induced apoptosis, although the phosphatase activity of calcineurin was not involved (Saeki *et al.*, 2007). Recently in the dimorphic basidiomycete, *Ustilago hordei*, single mutants of the calcineurin catalytic and regulatory subunits were generated and the Δ*cna1* strain exhibited sensitivity to NaCl and $CaCl_2$ stress but was more tolerant to EGTA and acetic acid when compared to the Δ*cnb1* strain (Cervantes-Chávez *et al.*, 2011). These results, coupled with our findings, suggest that CnaA and CnaB may be involved in other important roles besides functioning as a complex together. Specifically defining the domain responsible for localizing the calcineurin complex at the hyphal septum as well as the identification of other proteins associated with this complex are necessary to precisely understand the mechanistic basis for calcineurin signaling at the hyphal septum and how this is linked to establishing proper hyphal growth.

Experimental procedures

Strains, transformations and culture media

Strains used for transformations include isogenic *A. fumigatus* wild-type strain AF293, AF293.1 (*pyrG*⁻ uracil/uridine auxotroph) and AF293.6 (*pyrG*⁻ *argB*⁻ uracil/uridine and arginine auxotroph). *Escherichia coli* DH5α competent cells were used for subcloning experiments. *A. fumigatus* cultures were grown on glucose minimal medium (GMM) (Shimizu & Keller, 2001) at 37°C. Sabouraud dextrose medium (SDA) was used as high dextrose / low phosphate medium to test the growth of the calcineurin mutants. For some experiments, GMM was supplemented with 1.2 M sorbitol as osmotic support. Strains used in this study are listed in Table S1.

Construction of calcineurin deletion strains and complementation experiments

The *A. fumigatus* AF293.1 strain was used to create a single deletion strain of calcineurin B (Δ*cnaB*; Δ*cnaB*::*A. parasiticus pyrG*). AF293.6 strain was used to create the Δ*cnaA* Δ*cnaB* double deletion strain (Δ*cnaA* Δ*cnaB*; Δ*cnaA*::*A. fumigatus argB* and Δ*cnaB*::*A. parasiticus pyrG*). For generating the Δ*cnaB* strain, the 732 bp *A. fumigatus cnaB* gene (Afu6g04540) was replaced with the 3.1 kb *A. parasiticus pyrG* gene (Fig.1B). Approximately 1.0 kb of upstream flanking sequence and ~1.4 kb downstream flanking sequence of *cnaB* was cloned to flank the 3.1kb *A. parasiticus pyrG* gene in plasmid pJW24 (Steinbach et al., 2006) to create the replacement construct. The resulting replacement construct plasmid was used as a template to create the ~5.5 kb PCR amplicon for use in transformation. The AF293.1 (*pyrG*⁻) strain was transformed with the *cnaB* deletion construct and the transformants selected for growth in the absence of uracil/uridine supplementation.

For generating the Δ*cnaA* Δ*cnaB* strain, the *cnaA* deletion construct was made by cloning an ~1.8 kb upstream and downstream flanking sequences surrounding the ~1.9 kb *cnaA* gene into the plasmid, pLysB3 (Xue *et al.*, 2004). Next, the ~2.5 kb *argB* gene was excised from the plasmid, pArgB2 (Xue et al., 2004), and cloned between the *cnaA* flanking sequences. The resulting replacement construct plasmid was used as a template to create the ~6.1 kb PCR amplicon for use in transformation. The *cnaA* replacement construct was first transformed into the AF293.6 strain and the transformants were selected for growth in the absence of arginine supplementation. After screening the transformants for the homologous integration of the *cnaA* deletion construct by PCR and Southern analysis (Fig.1A), the Δ*cnaA*::*argB* strain (*pyrG*⁻Δ*cnaA*::*argB*) was retransformed with the cnaB::*pyrG* construct and selecting for growth in the absence of uracil/uridine supplementation to obtain the Δ*cnaA*::*argB* Δ*cnaB*::*pyrG* strain.

For complementation analysis of the Δ*cnaA* and Δ*cnaB* single mutants, the respective cDNA encoding *cnaA* and *cnaB* were separately cloned at the N-terminus of *egfp* in the plasmid pUCGH (a gift from Axel Brakhage) at a *Bam*HI site to obtain the *cnaA-egfp/cnaB-egfp* fusion constructs under the control of the *otef* promoter (Langfelder *et al.*, 2001) using the hygromycin B resistance gene (*hph*) as the selection marker. The plasmids pUCGH-*cnaA* and pUCGH-*cnaB* were transformed separately into their respective deletion strains to obtain the *cnaA* and *cnaB* complemented strains OCNAG3 and OCNBG2, respectively. CnaB cDNA was also cloned at the C-terminus of *mcherry* in the plasmid pUCNCR-phleo at the *Not*I site to obtain the *mcherry-cnaB* fusion construct under the control of the *otef* promoter, using the phleomycin resistance gene (*ble*) as the selection marker (pUCNCR-cnaB-phleo). The plasmid pUCNCR-phleo was constructed by replacing the *egfp* and hygromycin resistance gene with the 1.5 kb phleomycin resistance gene (Richie *et al.*, 2009) and N-terminal tagged *mcherry* (Addgene). For complementation of the Δ*cnaA* Δ*cnaB* strain, the plasmids pUCGH-*cnaA* and pUCNCR-*cnaB*-phleo were co-transformed into the

mutant and the tranformants were selected in the presence of 150 μg/ml hygromycin B and 125 μg/ml phleomycin. The obtained complemented strain was designated as OCNACB1. In all cases, the obtained transformants were verified for single copy integration by Southern analysis and utilized for further analysis by fluorescence microscopy. For generating the CnaB-EGFP expression strain in the *cnaA* deletion background and vice versa, the respective Δ*cnaA* and Δ*cnaB* strains were transformed with the plasmids pUCGH-*cnaB* and pUCGH-*cnaA*. The strains were designated as AKO-CNBG1 and BKO-CNAG2. In order to express *cnaA-egfp* and *mcherry-cnaB* under the control of their respective native promoters, a ~770 bp *cnaA* promoter and a ~565 bp *cnaB* promoter were amplified separately using the primers listed in Table S2 and cloned between the *Kpn*I and *Bam*HI sites in pUCGH (for *cnaA-egfp*) and the pUCNCR-phleo vectors (for *mcherry-cnaB*), respectively, to obtain the plasmids pUCGH-pCNA and pUCNCR-phleo-pCNB. In the next step the respective cDNAs encoding *cnaA* and *cnaB* were cloned at the *Bam*HI (in the case of *cnaA*) and *Not*I (in the case of *cnaB*) sites of pUCGH-pCNA and pUCNCR-phleo-pCNB to obtain the final constructs designated as pUCGH-NP-CNA and pUCNCR-NP-CNB. Additionally, a pUCGH-pCNB (harboring the native promoter of *cnaB*) and pUCGH-NP-CNB construct was also made by cloning the *cnaB* cDNA under its native promoter to express it as *cnaB-egfp*. Primers used in this study are listed in Table S2.

Construction of catalytic null mutant strains of calcineurin A in *A. fumigatus*

Site-directed mutagenesis of residues, Thr359 to Ser359 and Leu365 to Ser365, in the linker region between the catalytic domain and the CnaB-binding helix of CnaA was performed by using the primers listed in Table S2 and pUCGH-*cnaA* as a template. Briefly, the first PCR was done using complementary primers overlapping the regions to be mutated and the respective primers at the opposite ends to amplify two PCR fragments. Next, a fusion PCR was performed by using an equi-proportional mixture of the two PCR fragments as template and amplifying the mutated PCR fragment using the primers at the opposite ends (Table S2). Each fragment was then cloned into pUCGH-pCNA plasmid to obtain the final plasmids, pUCNP-CNA-T359P and and pUCNP-CNA-L365S. The constructs were verified by sequencing to confirm the respective mutation and then co-transformed along with the plasmid pUCNCR-phleo-pCNB into the Δ*cnaA* Δ*cnaB* strain to examine for complementation and localization of the mutated versions of CnaA. The complemented strains were designated as ABKO-CNAT359P-CNB-1 and ABKO-CNAL365S-CNB-1, respectively (Table S1).

Preparation of protein extracts and assay for calcineurin activity

To assay for calcineurin phosphatase activity the strains were cultured in GMM liquid medium for 48 h at 37°C and 250 rpm. Mycelia were harvested and washed in sterile distilled water and ~1-2 gm wet weight mycelia were homogenized using liquid nitrogen in a buffer containing 50 mM Tris-HCl, pH 7.4, 1 mM EGTA, 0.2% Triton X-100, 1 mM PMSF and 1:100 protease inhibitor cocktail. The homogenates were first centrifuged at 5,000 *g* for 10 min at 4°C to remove cell debris and collected supernatants were re-centrifuged at 20,000 *g* for 60 min at 4°C. Total protein in the extracts was estimated using the BioRad protein assay kit. Phosphatase activity of calcineurin in the protein extracts was assayed according to methods previously described (Pallen & Wang, 1983, Jayashree *et al.*, 2000), with minor modifications, by determining calmodulin-dependent protein phosphatase activity in the absence or in the presence of the inhibitor trifluoperazine (250 μM). Total reaction (100 μl) containing 25 mM Tris (pH 7.2), 25 mM MES (pH 7.0), 1 mM $MnCl_2$, 50 mM *p*-nitrophenyl phosphate, was incubated at 30°C for 10 min, and terminated by the addition of 10 μl of 13% (w/v) K_2HPO_4. The absorbance of the samples was measured immediately at 405 nM. The difference of absorbance values between the amounts of *p*-nitrophenol released in the absence and in the presence of trifluoperazine represented the

phosphatase activity mediated by calcineurin. One unit of enzyme activity is defined as nanomole of *p*-nitrophenol released from *p*-nitrophenyl phosphate per min per mg of protein.

Construction of calcineurin B truncations and site direct mutagenesis of calcineurin B

Truncated cDNA fragments of *cnaB* (Fig. 10), amplified by using pUCGH-*cnaB* as a template with primers listed in Table S2, were cloned into either pUCGH or pUCGH-pCNB separately. The respective constructs were sequenced to verify for the accuracy of truncations and transformed into the wild-type AF293 strain. Transformants selected in presence of hygromycin B were examined by fluorescence microscopy. The strains expressing truncated forms of CnaB in the wild-type background are listed in Table S1. The truncated *cnaB* construct, CnaB-tB-3, lacking the 4th Ca^{2+}-binding motif, was also transformed into the Δ*cnaB* strain to check for complementation. Another domain swapped construct, CnaB-SW2, was made by swapping the N-terminal sequence of CnaB (MEQP~DEVD) with the N-terminal sequence of human CnB1 (MGNE~DEIK). For this, the 5' region of human *CnB* encoding for the residues MEQP~DEVD was amplified by PCR using the plasmid, pET15b CnA CnB (obtained from Addgene), as a template using the primers listed in Table S2. The region encoding for the *A. fumigatus cnaB* sequence, RLRK~LSMF, was amplified by PCR using the plasmid, pUCGH-*cnaB*, as a template. The 2 PCR fragments were gel extracted, mixed in equal proportions, and a fusion PCR was performed to amplify the chimeric human *cnB* and *A. fumigatus cnaB* fragment (CnaB-SW2) using the primers listed in Table S2. The obtained CnaB-SW2 fragment was cloned into pUCGH, sequenced to verify for accuracy, and then transformed into the Δ*cnaB* strain to examine for complementation. The complemented strains were designated as OCNBG-tB3 and OCNBG-SW2, respectively (Table S1)

Point mutation of residues 15-ARRRA-20 to 15-AGGGGA-20, 44-RLRKR-48 to 44-AAAAA-48 and 51-KLDK-54 to 51-AAAA-54 at the N-terminus of CnaB was performed by using the primers listed in Table S2 and pUCGH-*cnaB* as a template. Briefly, the first PCR was done using complementary primers overlapping the regions to be mutated and the respective primers at the opposite ends to amplify two PCR fragments. Next, a fusion PCR was performed by using an equi-proportional mixture of the two PCR fragments as template and amplifying the mutated PCR fragment using the primers at the opposite ends (Table S2). Each fragment cloned into pUCGH was verified by sequencing to confirm the respective mutation and then transformed into the Δ*cnaB* strain to examine for complementation and localization of the mutated version of CnaB. The complemented strains were designated as OCNBG-RG, OCNBG-RA, and OCNBG-KA, respectively (Table S1).

Construction of Lifeact-RFP expression strains

In order to visualize actin network during growth and septation in *A. fumigatus*, the plasmid pAL10-Lifeact was obtained from the Fungal Genetics Stock Center (Kansas City). Actin network in *N. crassa* was previously visualized by using pAL10-Lifeact (Lichius & Read, 2010). pAL10-Lifeact was restriction digested with *Bam*HI and *Not*I to obtain a ~1.85 kb Lifeact-RFP fragment with the *trpC* terminator and cloned between the *Bam*HI and *Not*I sites in the pUCNG-phleo vector (Richie *et al.*, 2009) to obtain the final pUCO-LA-RFP-phleo vector for the expression of Lifeact-RFP under the control of *otef* promoter. This plasmid was transformed into the OCNAG3 strain to obtain the co-expression strain that is expressing both Lifeact-RFP and CnaA-EGFP. The plasmid pUCO-LA-RFP-phleo was also separately transformed into the Δ*cnaA* Δ*cnaB* strain to visualize actin network in the calcineurin deletion background. The obtained transformant strains were designated as OCNAG3-LARFP and ABKO-LARFP, respectively (Table S1).

Measurement of β-glucan and chitin contents

Aniline blue assay method was used to quantify 1,3-β-D-glucan content as described earlier (Steinbach *et al.*, 2007a). Briefly, conidia (10^6/ml) were cultured in GMM liquid medium for 48 h at 37°C and 250 rpm. Mycelial tissue was washed with 0.1 M NaOH and lyophilized. Five milligrams of lyophilized hyphal mat from each strain was resuspended in 250 μl of 1 M NaOH and sonicated for 30 sec, followed by incubation at 52°C for 30 min. After incubation, three 50-μl volumes from each sample were aliquoted into the wells of a masked, 96-well fluorescence plate. A volume of 185 μl of aniline blue mix (0.067% aniline blue, 0.35N HCl, 0.98 M glycine-NaOH, pH 9.5) was added to each well, and the plate was incubated for an additional 30 min at 52°C. The 96-well plate was then allowed to cool at room temperature for 30 min, and fluorescence readings were acquired on a SPECTRAmax M2 fluorimeter (Molecular Devices) at 405-nm excitation and 460-nm emission. To normalize values, a standard curve was created using curdlan, a β-1,3-glucan analog (Sigma). Relative fluorescence units were calculated from the best fit linear equation from the standard curve of defined curdlan amounts. Values were expressed as the relative fluorescence units per milligram of mycelial tissue, using the non-treated wild type as a control. The experiment was repeated three times. Final results represent the averages from three technical replicates. Statistical analyses were performed in Excel using the two-sample Student's *t* test assuming equal variances.

For chitin quantification, the growth and harvesting procedure of strains was similar to those described for 1,3-β-D-glucan measurement. Chitin assays were performed based on a slightly modified protocol (Lehmann & White, 1975) as previously described (Fortwendel et al., 2010). Briefly, 5 mg of lyophilized mycelial mat was resuspended in 3 ml of saturated KOH and incubated at 100-130°C for 1 h. After cooling to 25°C, 8 ml of ice-cold 75% ethanol was added. The resulting suspension was incubated in an ice bath for 15 min. A volume of 300 μl of a 13.3% (wt/vol) Celite 545 (C212; Fisher Chemicals) suspension was added, and the tubes were centrifuged at $1,500 \times g$ for 5 min at 2°C. Pellets were washed once with 10 ml of ice-cold 40% ethanol, followed by two washes in 10 ml ice-cold water, with centrifuging as before. To normalize values, a standard curve was created using serial dilution of glucosamine. The final pellet from each sample was resuspended in 0.5 ml of water. 0.5 ml of 5% (wt/vol) $NaNO_2$, and 0.5 ml of 5% (wt/vol) $KHSO_4$ was added to each tube. For controls, 0.2 ml of both $NaNO_2$ and $KHSO_4$ were added. All tubes were gently mixed three times for a 15-min period, followed by centrifugation at $1,500 \times g$ for 2 min at 2°C. Aliquots (150 μl each) were removed from each supernatant and added to 450 μl of water in a new tube. A volume of 0.2 ml of 12.5% (wt/vol) NH_4 sulfamate was added to each tube and mixed vigorously each minute for 5 min, followed by the addition of 0.2 ml of 3-methylbenzthiazolinone-2-hydrazone (5 mg/ml) and incubation at 100-130°C for 3 min. Tubes were allowed to cool, and 0.2 ml of 0.83% (wt/vol) ferric chloride was added, followed by incubation at room temperature for 25 min. Absorbance was read at 650 nm on a Nanodrop ND-1000 spectrophotometer. Concentrations of glucosamine in the final supernatant were calculated from the best fit linear trend line equation of the defined glucosamine standard curves. Chitin levels were reported as glucosamine equivalents (in micrograms/milliliter) per mg of lyophilized tissue assayed. Final results represent the averages from three independent experiments. Statistical analyses were performed in Excel using the two-sample Student's *t* test assuming equal variances.

Protein extraction and Western analysis

The strains expressing CnaB-EGFP fusion constructs were grown in GMM liquid medium as shaking cultures for a period of 24 h at 37°C. Cell extracts were prepared by homogenizing the mycelia using liquid nitrogen in buffer A (50 mM Tris-HCl, pH 7.5, 150 mM NaCl, 50 mM KCl, 0.01% Triton X-100, 1 mM PMSF and 1:100 protease inhibitor

cocktail). Total cell lysate was initially centrifuged at 1200 rpm to eliminate the cell debris, and the supernatant obtained was further centrifuged (5000 rpm, 10 min at 4°C). The final supernatant and pellet fractions were collected and approximately 50 μg of total protein were resolved by electrophoresis through a 12% SDS-polyacrylamide gel using a Miniprotean electrophoresis cell (Bio-Rad). The proteins were electroblotted onto a polyvinylidene difluoride membrane (Bio-Rad) and probed with polyclonal rabbit anti-GFP as primary antibody. Peroxidase-labeled rabbit anti-IgG (Rockland) was used as a secondary antibody. Detection was carried out using SuperSignal West Pico chemiluminescent substrate (Thermo Scientific).

Calcofluor white and Aniline blue staining

Calcofluor white staining of the wild type and calcineurin deletion strains was performed by culturing 10^4 conidia in coverslips immersed in 10 ml GMM medium and grown for 24 h at 37°C. The coverslips were rinsed in sterile water and inverted onto a 200 μl drop of calcofluor white staining solution for 5 min at 25°C. Coverslips were then rinsed twice for 10 min in sterile water and observed by fluorescence microscopy.

Staining of cell wall β-glucan with aniline blue was performed by growing the various strains as mentioned for calcofluor white staining. The coverslips were rinsed in sterile water and inverted onto a 200 μl drop of aniline blue (0.1 mg/ml) staining solution for 5 min at 25°C. Stained mycelia were directly observed by fluorescence microscopy.

Nuclear staining

The strains were grown in GMM liquid medium on coverslips for 18-20 h and stained with propidium iodide. Briefly, the cultures were washed in 50 mM PIPES (pH 6.7) for 5 min, fixed in 8% formaldehyde with 0.2% Triton X-100 for 40 min at 25°C, washed in 50 mM PIPES (pH 6.7) for 10 min and treated with RNase (100 μg/ml) for 60 min at 37°C. After washing with 50 mM PIPES (pH 6.7) for 10 min the fixed sample was stained with propidium iodide solution (12.5 μg/ml) in 50 mM PIPES (pH 6.7) for 5 min and observed under the fluorescence microscope.

Electron Microscopy

For SEM of the calcineurin mutants, 10^4 conidia of each strain were inoculated into 10 ml GMM medium in a petri dish containing sterile 22×22 mm (No. 2) coverslips and grown for 48 h at 37°C. The wild-type and all the complemented strains were grown for 24 h at 37°C. The mycelia on the coverslips were fixed with 50 mM PIPES buffer (pH 7) containing 3.5% formaldehyde for 60 min and washed three times for 10 min each. The fixed mycelia were then treated consecutively with 50, 70 and 90% ethanol for 10 min each. Final treatment was done with 99.5% ethanol three times for 10 min each. The coverslips were then allowed to dry in a laminar hood overnight. The fixed and dried mycelial samples were then sputter coated with gold and observed on an FE-SEM (FEI model XL-30) using an accelerating voltage of 7kV.

For TEM of the wild-type and the calcineurin mutants, 10^4 conidia of each strain were inoculated into 10 ml GMM medium and grown for 48 h at 37°C. After 48 h of growth the mycelial pellets were washed three times in distilled water and fixed in 5% glutaraldehyde in 0.1M cocodylate buffer. The mycelia were embedded in low viscosity Spurrs resin and ultrathin sectioning was performed. The sections were then stained with uranyl acetate and lead citrate. Images were obtained on Zeiss EM900 electron microscope and negatives were scanned for image analysis.

Fluorescence microscopy and time-lapse imaging

Conidia (10^4) of the strains were inoculated in 500 μl of GMM medium on sterile coverslips (22×60 mm; No.1). After culturing for a period of 18-20 h at 37° C the strains were observed by fluorescence microscopy using an Axioskop 2 plus microscope (Zeiss) equipped with AxioVision 4.6 imaging software.

For live cell imaging experiments carried out to monitor the localization of calcineurin during germination, hyphal growth and septation in the *cnaA*-EGFP expression strain, 10^2 conidia were inoculated into a 35 mm cover glass bottom petri dish (Matek) in a total volume of 500 μl GMM broth and incubated at 37°C for 3 h. The dish was then shifted to a Zeiss Axio Observer Z1 motorized live cell station equipped with a Pecon XL S1 incubator (temperature controlled at 37°C). Differential interference contrast (DIC) and GFP-fluorescent images during conidial germination and hyphal growth were captured at 5 min intervals over a period of 15 h using the 63x/1.4 oil Plan Apochromat DIC objective and GFP filtercube HE38 with a Coolsnap ES2 high resolution CCD camera. Images were collected and movies were made using the MetaMorph 7.6.5 analysis software.

Supplementary Material

Refer to Web version on PubMed Central for supplementary material.

Acknowledgments

References

Aramburu J, Rao A, Klee CB. Calcineurin: from structure to function. Curr Top Cell Regul. 2000; 36:237–295. [PubMed: 10842755]

Bader T, Bodendorfer B, Schroppel K, Morschhauser J. Calcineurin Is Essential for Virulence in *Candida albicans*. Infect. Immun. 2003; 71:5344–5354. [PubMed: 12933882]

Bader T, Schroppel K, Bentink S, Agabian N, Kohler G, Morschhauser J. Role of Calcineurin in Stress Resistance, Morphogenesis, and Virulence of a *Candida albicans* Wild-Type Strain. Infect. Immun. 2006; 74:4366–4369. [PubMed: 16790813]

Bonilla M, Nastase KK, Cunningham KW. Essential role of calcineurin in response to endoplasmic reticulum stress. EMBO J. 2002; 21:2343–2353. [PubMed: 12006487]

Cameron AM, Steiner JP, Roskams AJ, Ali SM, Ronnettt GV, Snyder SH. Calcineurin associated with the inositol 1,4,5-trisphosphate receptor-FKBP12 complex modulates Ca2+ flux. Cell. 1995; 83:463–472. [PubMed: 8521476]

Cervantes-Chávez JA, Ali S, Bakkeren G. Response to Environmental Stresses, Cell-wall Integrity, and Virulence Are Orchestrated Through the Calcineurin Pathway in *Ustilago hordei*. Molecular Plant-Microbe Interactions. 2011; 24:219–232. [PubMed: 20977307]

Chen S, Song Y, Cao J, Wang G, Wei H, Xu X, Lu L. Localization and function of calmodulin in live-cells of *Aspergillus nidulans*. Fungal Genetics and Biology. 2010a; 47:268–278. [PubMed: 20034586]

Chen YL, Kozubowski L, Cardenas ME, Heitman J. On the Roles of Calcineurin in Fungal Growth and Pathogenesis. Curr Fungal Infect Rep. 2010b; 4:244–255.

Choi J, Kim Y, Kim S, Park J, Lee Y-H. MoCRZ1, a gene encoding a calcineurin-responsive transcription factor, regulates fungal growth and pathogenicity of *Magnaporthe oryzae*. Fungal Genetics and Biology. 2009; 46:243–254. [PubMed: 19111943]

Clipstone NA, Fiorentino DF, Crabtree GR. Molecular analysis of the interaction of calcineurin with drug-immunophilin complexes. Journal of Biological Chemistry. 1994; 269:26431–26437. [PubMed: 7523407]

Cohen P, Cohen PT. Protein phosphatases come of age. Journal of Biological Chemistry. 1989; 264:21435–21438. [PubMed: 2557326]

Cramer RA Jr. Perfect BZ, Pinchai N, Park S, Perlin DS, Asfaw YG, Heitman J, Perfect JR, Steinbach WJ. Calcineurin target CrzA regulates conidial germination, hyphal growth, and pathogenesis of *Aspergillus fumigatus*. Eukaryot Cell. 2008; 7:1085–1097. [PubMed: 18456861]

Cruz MC, Goldstein AL, Blankenship JR, Del Poeta M, Davis D, Cardenas ME, Perfect JR, McCusker JH, Heitman J. Calcineurin is essential for survival during membrane stress in *Candida albicans*. EMBO J. 2002; 21:546–559. [PubMed: 11847103]

Cyert MS. Genetic analysis of calmodulin and its targets in *Saccharomyces cerevisiae*. Annual Review of Genetics. 2001; 35:647–672.

Cyert MS. Calcineurin signaling in *Saccharomyces cerevisiae*: how yeast go crazy in response to stress. Biochemical and Biophysical Research Communications. 2003; 311:1143–1150. [PubMed: 14623300]

Cyert MS, Kunisawa R, Kaim D, Thorner J. Yeast has homologs (CNA1 and CNA2 gene products) of mammalian calcineurin, a calmodulin-regulated phosphoprotein phosphatase. Proceedings of the National Academy of Sciences of the United States of America. 1991; 88:7376–7380. [PubMed: 1651503]

Cyert MS, Thorner J. Regulatory subunit (CNB1 gene product) of yeast Ca^{2+}/calmodulin-dependent phosphoprotein phosphatases is required for adaptation to pheromone. Mol. Cell. Biol. 1992; 12:3460–3469. [PubMed: 1321337]

da Silva Ferreira ME, Heinekamp T, Hartl A, Brakhage AA, Semighini CP, Harris SD, Savoldi M, de Gouvea PF, de Souza Goldman MH, Goldman GH. Functional characterization of the *Aspergillus fumigatus* calcineurin. Fungal Genet Biol. 2007; 44:219–230. [PubMed: 16990036]

Delgado-Jarana J, Sousa S, Gonzalez F, Rey M, Llobell A. ThHog1 controls the hyperosmotic stress response in *Trichoderma harzianum*. Microbiology. 2006; 152:1687–1700. [PubMed: 16735732]

Feske S, Okamura H, Hogan PG, Rao A. Ca^{2+}/calcineurin signalling in cells of the immune system. Biochemical and Biophysical Research Communications. 2003; 311:1117–1132. [PubMed: 14623298]

Fortwendel JR, Juvvadi PR, Perfect BZ, Rogg LE, Perfect JR, Steinbach WJ. Transcriptional regulation of chitin synthases by calcineurin controls paradoxical growth of *Aspergillus fumigatus* in response to caspofungin. Antimicrob Agents Chemother. 2010; 54:1555–1563. [PubMed: 20124000]

Fortwendel JR, Juvvadi PR, Pinchai N, Perfect BZ, Alspaugh JA, Perfect JR, Steinbach WJ. Differential effects of inhibiting chitin and 1,3-{beta}-D-glucan synthesis in ras and calcineurin mutants of *Aspergillus fumigatus*. Antimicrob Agents Chemother. 2009; 53:476–482. [PubMed: 19015336]

Fox DS, Cox GM, Heitman J. Phospholipid-Binding Protein Cts1 Controls Septation and Functions Coordinately with Calcineurin in *Cryptococcus neoformans*. Eukaryotic Cell. 2003; 2:1025–1035. [PubMed: 14555485]

Fox DS, Cruz MC, Sia RAL, Ke H, Cox GM, Cardenas ME, Heitman J. Calcineurin regulatory subunit is essential for virulence and mediates interactions with FKBP12–FK506 in *Cryptococcus neoformans*. Molecular Microbiology. 2001; 39:835–849. [PubMed: 11251806]

Fox DS, Heitman J. Good fungi gone bad: The corruption of calcineurin. BioEssays. 2002; 24:894–903. [PubMed: 12325122]

Fox H, Hickey PC, Fernández-Ábalos JM, Lunness P, Read ND, Doonan JH. Dynamic distribution of BIMGPP1 in living hyphae of Aspergillus indicates a novel role in septum formation. Molecular Microbiology. 2002; 45:1219–1230. [PubMed: 12207691]

Fukuda K, Yamada K, Deoka K, Yamashita S, Ohta A, Horiuchi H. Class III Chitin Synthase ChsB of *Aspergillus nidulans* Localizes at the Sites of Polarized Cell Wall Synthesis and Is Required for Conidial Development. Eukaryotic Cell. 2009; 8:945–956. [PubMed: 19411617]

Garrett-Engele P, Moilanen B, Cyert M. Calcineurin, the Ca^{2+}/calmodulin-dependent protein phosphatase, is essential in yeast mutants with cell integrity defects and in mutants that lack a functional vacuolar H(+)-ATPase. Mol. Cell. Biol. 1995; 15:4103–4114. [PubMed: 7542741]

Harel A, Bercovich S, Yarden O. Calcineurin Is Required for Sclerotial Development and Pathogenicity of *Sclerotinia sclerotiorum* in an Oxalic Acid-Independent Manner. Molecular Plant-Microbe Interactions. 2006; 19:682–693. [PubMed: 16776301]

Heath VL, Shaw SL, Roy S, Cyert MS. Hph1p and Hph2p, Novel Components of Calcineurin-Mediated Stress Responses in *Saccharomyces cerevisiae*. Eukaryotic Cell. 2004; 3:695–704. [PubMed: 15189990]

Hemenway C, Heitman J. Calcineurin. Cell Biochemistry and Biophysics. 1999; 30:115–151. [PubMed: 10099825]

Higuchi S, Tamura J, Giri PR, Polli JW, Kincaid RL. Calmodulin-dependent protein phosphatase from *Neurospora crassa*. Molecular cloning and expression of recombinant catalytic subunit. Journal of Biological Chemistry. 1991; 266:18104–18112. [PubMed: 1655737]

Ichinomiya M, Yamada E, Yamashita S, Ohta A, Horiuchi H. Class I and Class II Chitin Synthases Are Involved in Septum Formation in the Filamentous Fungus *Aspergillus nidulans*. Eukaryotic Cell. 2005; 4:1125–1136. [PubMed: 15947204]

Ito A, Hashimoto T, Hirai M, Takeda T, Shuntoh H, Kuno T, Tanaka C. The complete primary structure of calcineurin A, a calmodulin binding protein homologous with protein phosphatases 1 and 2A. Biochemical and Biophysical Research Communications. 1989; 163:1492–1497. [PubMed: 2551293]

Jayashree T, Praveen Rao J, Subramanyam C. Regulation of aflatoxin production by Ca^{2+}/calmodulin-dependent protein phosphorylation and dephosphorylation. FEMS Microbiology Letters. 2000; 183:215–219. [PubMed: 10675586]

Jiang B, Cyert MS. Identification of a Novel Region Critical for Calcineurin Function in Vivo and in Vitro. Journal of Biological Chemistry. 1999; 274:18543–18551. [PubMed: 10373463]

Jiang G, Wei Q. Function and structure of N-terminal and C-terminal domains of calcineurin B subunit. Biol Chem. 2003; 384:1299–1303. [PubMed: 14515992]

Jiménez-Vidal M, Srivastava J, Putney LK, Barber DL. Nuclear-localized Calcineurin Homologous Protein CHP1 Interacts with Upstream Binding Factor and Inhibits Ribosomal RNA Synthesis. Journal of Biological Chemistry. 2010; 285:36260–36266. [PubMed: 20720019]

Juvvadi PR, Fortwendel JR, Pinchai N, Perfect BZ, Heitman J, Steinbach WJ. Calcineurin Localizes to the Hyphal Septum in *Aspergillus fumigatus*: Implications for Septum Formation and Conidiophore Development. Eukaryotic Cell. 2008; 7:1606–1610. [PubMed: 18606829]

Juvvadi PR, Kuroki Y, Arioka M, Nakajima H, Kitamoto K. Functional analysis of the calcineurin-encoding gene cnaA from *Aspergillus oryzae*: evidence for its putative role in stress adaptation. Arch Microbiol. 2003; 179:416–422. [PubMed: 12709783]

Kafadar KA, Cyert MS. Integration of Stress Responses: Modulation of Calcineurin Signaling in *Saccharomyces cerevisiae* by Protein Kinase A. Eukaryotic Cell. 2004; 3:1147–1153. [PubMed: 15470242]

Kakalis LT, Kennedy M, Sikkink R, Rusnak F, Armitage IM. Characterization of the calcium-binding sites of calcineurin B. FEBS Letters. 1995; 362:55–58. [PubMed: 7698353]

Kita A, Sugiura R, Shoji H, He Y, Deng L, Lu Y, Sio SO, Takegawa K, Sakaue M, Shuntoh H, Kuno T. Loss of Apm1, the {micro}1 Subunit of the Clathrin-Associated Adaptor-Protein-1 Complex, Causes Distinct Phenotypes and Synthetic Lethality with Calcineurin Deletion in Fission Yeast. Mol. Biol. Cell. 2004; 15:2920–2931. [PubMed: 15047861]

Kothe GO, Free SJ. Calcineurin Subunit B Is Required for Normal Vegetative Growth in *Neurospora crassa*. Fungal Genetics and Biology. 1998; 23:248–258. [PubMed: 9680955]

Kraus PR, Heitman J. Coping with stress: calmodulin and calcineurin in model and pathogenic fungi. Biochemical and Biophysical Research Communications. 2003; 311:1151–1157. [PubMed: 14623301]

Kretsinger RH. Structure and evolution of calcium-modulated proteins. CRC Crit Rev Biochem. 1980; 8:119–174. [PubMed: 6105043]

la Cour T, Kiemer L, Mølgaard A, Gupta R, Skriver K, Brunak S. Analysis and prediction of leucine-rich nuclear export signals. Protein Engineering Design and Selection. 2004; 17:527–536.

Lagorce A, Hauser NC, Labourdette D, Rodriguez C, Martin-Yken H, Arroyo J, Hoheisel JD, François J. Genome-wide Analysis of the Response to Cell Wall Mutations in the Yeast *Saccharomyces cerevisiae*. Journal of Biological Chemistry. 2003; 278:20345–20357. [PubMed: 12644457]

Langfelder K, Philippe B, Jahn B, Latge J-P, Brakhage AA. Differential Expression of the *Aspergillus fumigatus* pksP Gene Detected In Vitro and In Vivo with Green Fluorescent Protein. Infect. Immun. 2001; 69:6411–6418. [PubMed: 11553585]

Lehmann PF, White LO. Chitin assay used to demonstrate renal localization and cortisone-enhanced growth of *Aspergillus fumigatus* mycelium in mice. Infect. Immun. 1975; 12:987–992. [PubMed: 1104488]

Li H, Wei Q. Conformation changes in brain calcineurin in diabetic rats with or without treatment with vanadyl sulfate. IUBMB Life. 2001; 51:373–376. [PubMed: 11758805]

Li J, Jia Z, Zhou W, Wei Q. Calcineurin regulatory subunit B is a unique calcium sensor that regulates calcineurin in both calcium-dependent and calcium-independent manner. Proteins. 2009; 77:612–623. [PubMed: 19536897]

Li W, Handschumacher RE. Identification of two calcineurin B-binding proteins: tubulin and heat shock protein 60. Biochim. Biophys. Acta. 2002; 1599:72–81. [PubMed: 12479407]

Lichius A, Read ND. A versatile set of Lifeact-RFP expression plasmids for live-cell imaging of F-actin in filamentous fungi. Fungal Genetics Reports. 2010; 57:8–14.

Lu Y, Sugiura R, Yada T, Cheng H, Sio SO, Shuntoh H, Kuno T. Calcineurin is implicated in the regulation of the septation initiation network in fission yeast. Genes to Cells. 2002; 7:1009–1019. [PubMed: 12354095]

Martin BA, Oxhorn BC, Rossow CR, Perrino BA. A Cluster of Basic Amino Acid Residues in Calcineurin B Participates in the Binding of Calcineurin to Phosphatidylserine Vesicles. Journal of Biochemistry. 2001; 129:843–849. [PubMed: 11328610]

Mendoza I, Quintero FJ, Bressan RA, Hasegawa PM, Pardo JM. Activated Calcineurin Confers High Tolerance to Ion Stress and Alters the Budding Pattern and Cell Morphology of Yeast Cells. Journal of Biological Chemistry. 1996; 271:23061–23067. [PubMed: 8798496]

Merat DL, Hu ZY, Carter TE, Cheung WY. Bovine brain calmodulin-dependent protein phosphatase. Regulation of subunit A activity by calmodulin and subunit B. Journal of Biological Chemistry. 1985; 260:11053–11059. [PubMed: 2993300]

Moser M, Geiser J, Davis T. Ca^{2+}-calmodulin promotes survival of pheromone-induced growth arrest by activation of calcineurin and Ca^{2+}-calmodulin-dependent protein kinase. Mol. Cell. Biol. 1996; 16:4824–4831. [PubMed: 8756641]

Nagita M, Inoue H, Nakamura N, Kanazawa H. Two Nuclear Export Signals Specify the Cytoplasmic Localization of Calcineurin B Homologous Protein 1. Journal of Biochemistry. 2003; 134:919–925. [PubMed: 14769882]

Nakamura T, Liu Y, Hirata D, Namba H, Harada S, Hirokawa T, Miyakawa T. Protein phosphatase type 2B (calcineurin)-mediated, FK506-sensitive regulation of intracellular ions in yeast is an important determinant for adaptation to high salt stress conditions. EMBO J. 1993; 12:4063–4071. [PubMed: 7693452]

Odom A, Muir S, Lim E, Toffaletti DL, Perfect J, Heitman J. Calcineurin is required for virulence of *Cryptococcus neoformans*. EMBO J. 1997; 16:2576–2589. [PubMed: 9184205]

Pallen CJ, Wang JH. Calmodulin-stimulated dephosphorylation of *p*-nitrophenyl phosphate and free phosphotyrosine by calcineurin. Journal of Biological Chemistry. 1983; 258:8550–8553. [PubMed: 6190810]

Perrino BA, Ng LY, Soderling TR. Calcium Regulation of Calcineurin Phosphatase Activity by Its B Subunit and Calmodulin. Journal of Biological Chemistry. 1995; 270:340–346. [PubMed: 7814394]

Prokisch H, Yarden O, Dieminger M, Tropschug M, Barthelmess IB. Impairment of calcineurin function in *Neurospora crassa* reveals its essential role in hyphal growth, morphology and maintenance of the apical Ca^{2+} gradient. Mol Gen Genet. 1997; 256:104–114. [PubMed: 9349701]

Rasmussen C, Garen C, Brining S, Kincaid RL, Means RL, Means AR. The calmodulin-dependent protein phosphatase catalytic subunit (calcineurin A) is an essential gene in *Aspergillus nidulans*. EMBO J. 1994; 13:3917–3924. [PubMed: 8070419]

Reedy JL, Filler SG, Heitman J. Elucidating the *Candida albicans* calcineurin signaling cascade controlling stress response and virulence. Fungal Genetics and Biology. 2010; 47:107–116. [PubMed: 19755168]

Richie DL, Hartl L, Aimanianda V, Winters MS, Fuller KK, Miley MD, White S, McCarthy JW, Latgé J-P, Feldmesser M, Rhodes JC, Askew DS. A Role for the Unfolded Protein Response (UPR) in Virulence and Antifungal Susceptibility in *Aspergillus fumigatus*. PLoS Pathog. 2009; 5:e1000258. [PubMed: 19132084]

Rusnak F, Mertz P. Calcineurin: Form and Function. Physiological Reviews. 2000; 80:1483–1521. [PubMed: 11015619]

Saeki M, Irie Y, Ni L, Itsuki Y, Terao Y, Kawabata S, Kamisaki Y. Calcineurin Potentiates the Activation of Procaspase-3 by Accelerating Its Proteolytic Maturation. Journal of Biological Chemistry. 2007; 282:11786–11794. [PubMed: 17324936]

Shimizu K, Keller NP. Genetic Involvement of a cAMP-Dependent Protein Kinase in a G Protein Signaling Pathway Regulating Morphological and Chemical Transitions in *Aspergillus nidulans*. Genetics. 2001; 157:591–600. [PubMed: 11156981]

Sigal CT, Zhou W, Buser CA, McLaughlin S, Resh MD. Amino-terminal basic residues of Src mediate membrane binding through electrostatic interaction with acidic phospholipids. Proceedings of the National Academy of Sciences of the United States of America. 1994; 91:12253–12257. [PubMed: 7527558]

Stathopoulos-Gerontides A, Guo JJ, Cyert MS. Yeast calcineurin regulates nuclear localization of the Crz1p transcription factor through dephosphorylation. Genes & Development. 1999; 13:798–803. [PubMed: 10197980]

Steinbach WJ, Cramer RA Jr. Perfect BZ, Asfaw YG, Sauer TC, Najvar LK, Kirkpatrick WR, Patterson TF, Benjamin DK Jr. Heitman J, Perfect JR. Calcineurin controls growth, morphology, and pathogenicity in *Aspergillus fumigatus*. Eukaryot Cell. 2006; 5:1091–1103. [PubMed: 16835453]

Steinbach WJ, Cramer RA Jr. Perfect BZ, Henn C, Nielsen K, Heitman J, Perfect JR. Calcineurin inhibition or mutation enhances cell wall inhibitors against *Aspergillus fumigatus*. Antimicrob Agents Chemother. 2007a; 51:2979–2981. [PubMed: 17502415]

Steinbach WJ, Reedy JL, Cramer RA Jr. Perfect JR, Heitman J. Harnessing calcineurin as a novel anti-infective agent against invasive fungal infections. Nat Rev Microbiol. 2007b; 5:418–430. [PubMed: 17505522]

Stewart AA, Ingebritsen TS, Manalan A, Klee CB, Cohen P. Discovery of A Ca^{2+}-and calmodulin-dependent protein phosphatase. FEBS Letters. 1982; 137:80–84. [PubMed: 6279434]

Sugiura R, Sio SO, Shuntoh H, Kuno T. Calcineurin phosphatase in signal transduction: lessons from fission yeast. Genes to Cells. 2002; 7:619–627. [PubMed: 12081640]

Teepe AG, Loprete DM, He Z, Hoggard TA, Hill TW. The protein kinase C orthologue PkcA plays a role in cell wall integrity and polarized growth in *Aspergillus nidulans*. Fungal Genetics and Biology. 2007; 44:554–562. [PubMed: 17118679]

Wang YL, Wang Y, Tong L, Wei Q. Overexpression of calcineurin B subunit (CnB) enhances the oncogenic potential of HEK293 cells. Cancer Sci. 2008; 99:1100–1108. [PubMed: 18422742]

Wei Q, Lu ZJ, Xiao FX, Xing LZ, Li DH. A useful method of calcineurin, calmodulin, and other calcium binding proteins. Chin. Biochem. J. 1993; 9:6–10.

Wen W, Meinkotht JL, Tsien RY, Taylor SS. Identification of a signal for rapid export of proteins from the nucleus. Cell. 1995; 82:463–473. [PubMed: 7634336]

West S, Bamborough P, Tully R. Tertiary structure of calcineurin B by homology modeling. Journal of Molecular Graphics. 1993; 11:47–52. [PubMed: 8388712]

Xue T, Nguyen CK, Romans A, Kontoyiannis DP, May GS. Isogenic auxotrophic mutant strains in the *Aspergillus fumigatus* genome reference strain AF293. Archives of Microbiology. 2004; 182:346–353. [PubMed: 15365692]

Yada T, Sugiura R, Kita A, Itoh Y, Lu Y, Hong Y, Kinoshita T, Shuntoh H, Kuno T. Its8, a Fission Yeast Homolog of Mcd4 and Pig-n, Is Involved in GPI Anchor Synthesis and Shares an Essential Function with Calcineurin in Cytokinesis. Journal of Biological Chemistry. 2001; 276:13579–13586. [PubMed: 11297516]

Yoshida T, Toda T, Yanagida M. A calcineurin-like gene ppb1+ in fission yeast: mutant defects in cytokinesis, cell polarity, mating and spindle pole body positioning. J Cell Sci. 1994; 107:1725–1735. [PubMed: 7983142]

Zhang Y, Sugiura R, Lu Y, Asami M, Maeda T, Itoh T, Takenawa T, Shuntoh H, Kuno T. Phosphatidylinositol 4-Phosphate 5-Kinase Its3 and Calcineurin Ppb1 Coordinately Regulate Cytokinesis in Fission Yeast. Journal of Biological Chemistry. 2000; 275:35600–35606. [PubMed: 10950958]

Zhu J, McKeon F. NF-AT activation requires suppression of Crm1-dependent export by calcineurin. Nature. 1999; 398:256–260. [PubMed: 10094050]
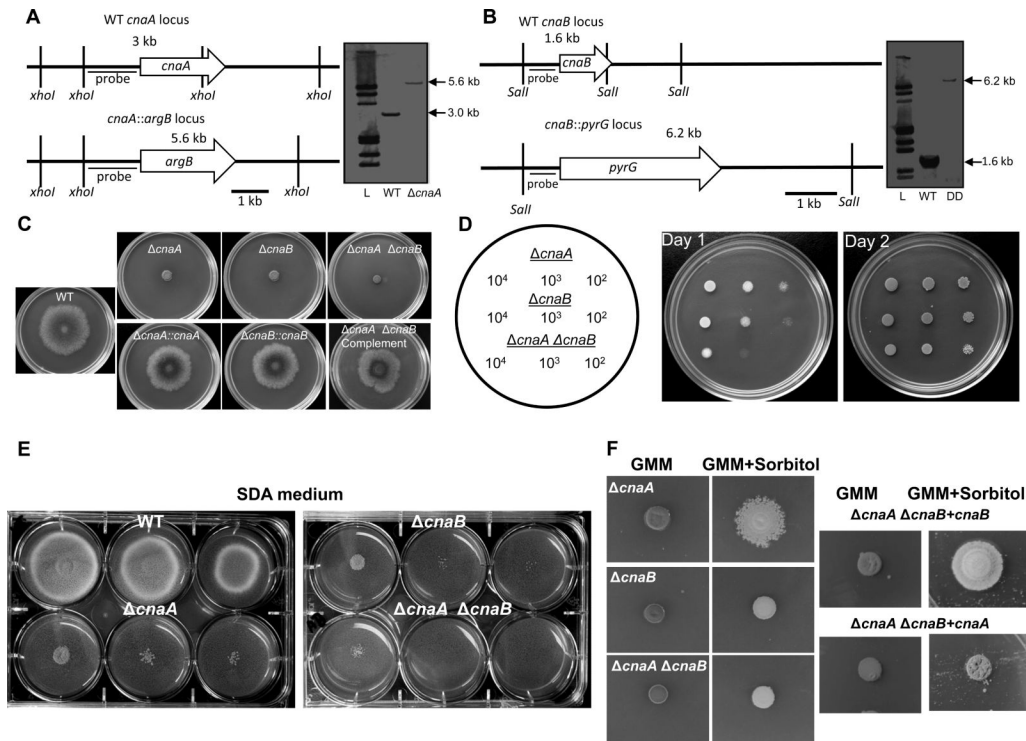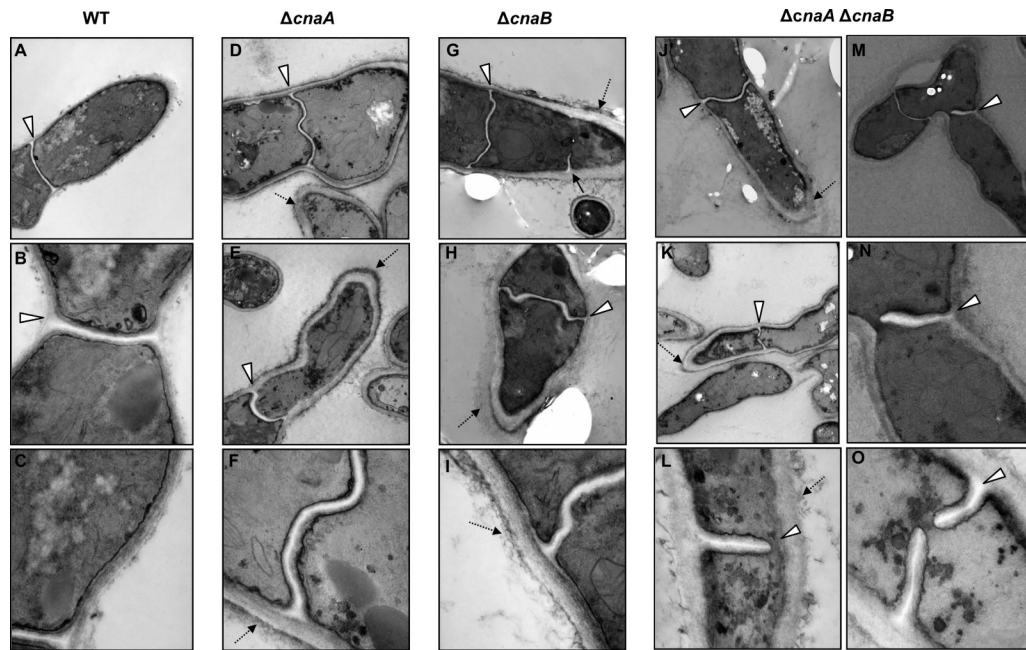
Figure 1.

Construction of the *cnaA* and *cnaB* deletion strains in *A. fumigatus* and radial growth analysis of the calcineurin mutants. (A) Schematic representation of the genomic locus of the WT and the *cnaA* and *cnaB* deletion strains. The entire coding sequence of the *A. fumigatus cnaA* gene was replaced with the *A. fumigatus argB* gene by homologous recombination. Southern analysis with *xho*I-digested genomic DNA and *cnaA* left flank probe shows the replacement of *cnaA* by *argB* as a 5.6 kb fragment in the Δ*cnaA* strain. (B) Genomic DNA from both the wild type and the Δ*cnaA* Δ*cnaB* strains was digested with *Sal*I; The DIG-labeled probe bound to a 1.6 kb and a 6.2 kb band in the wild type and the Δ*cnaA* Δ*cnaB* strains, respectively, showing the replacement of *cnaB* by *A. parasiticus pyrG* as a 6.2 kb fragment in the Δ*cnaA* strain. (C). Radial growth of the wild-type, the calcineurin single mutants (Δ*cnaA* and Δ*cnaB*) and the double mutant Δ*cnaA* Δ*cnaB* strain, and the corresponding complemented strains over a period of 3 days at 37°C on GMM agar medium. A total of 1×10^4 conidia were spotted for each strain. (D) Different concentrations of inocula as indicated were spotted on GMM agar plates and growth of the strains was monitored over a period of 2 days at 37°C to observe the severe growth defect of the Δ*cnaA* Δ*cnaB* strain in comparison to the single mutants. (E). Different concentrations of inocula were spotted on SDA plates and growth of the strains was monitored over a period of 3 days at 37°C to observe the growth defect of the calcineurin mutants. (F). A total of 1×10^5 conidia from each calcineurin mutant were spotted on GMM agar supplemented with 1.2 M sorbitol and observed for growth remediation over a period of 3 days at 37°C. Sorbitol-dependent partial growth remediation in the absence of CnaA may be noted in the Δ*cnaA* and Δ*cnaA* Δ*cnaB* + *cnaB* strains.
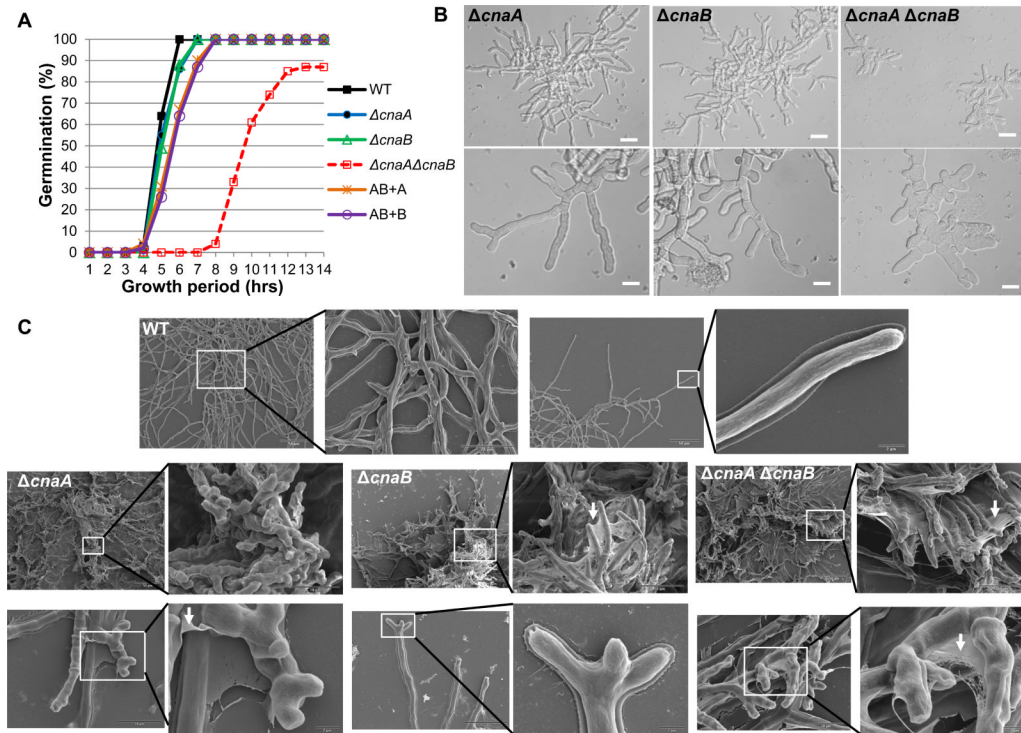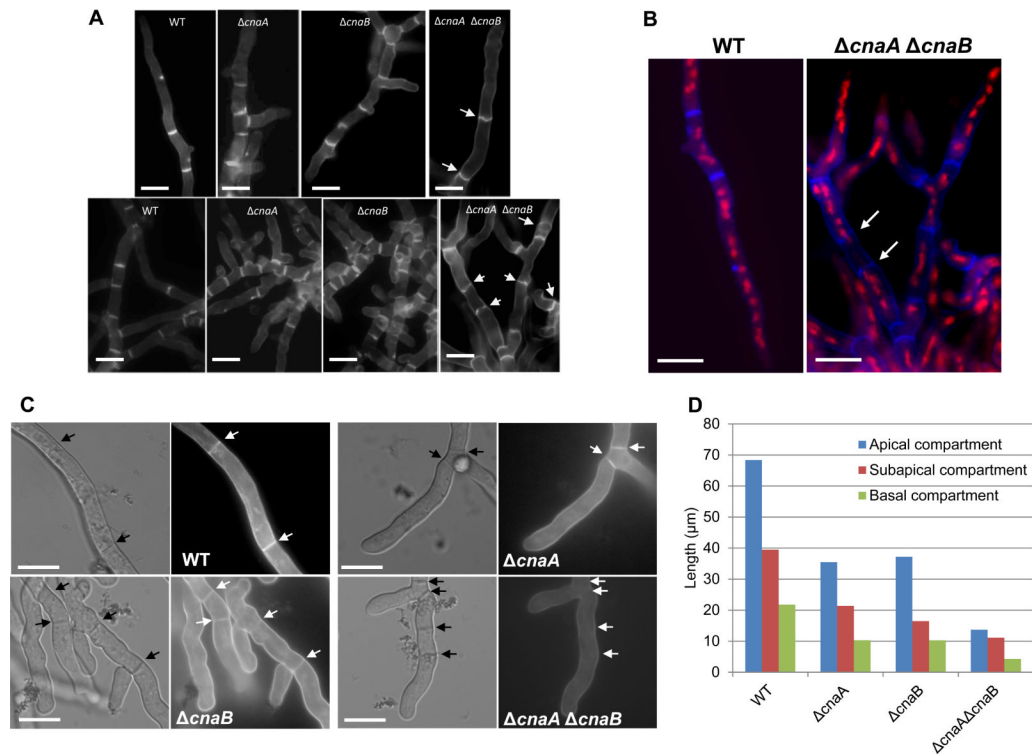
Figure 2.
Germination and hyphal growth phenotypes of the calcineurin mutants. (A). Comparison and quantitative analysis of germination of the wild type and the calcineurin mutant strains over the first 14 h of growth at 37°C. A total of 1×10^4 conidia from the wild type and each calcineurin mutant were inoculated into 10 ml GMM broth in a petri dish with coverslips. At hourly intervals, coverslips were taken out and each time a total of 100 conidia were counted and each time point represents the percentage of germlings observed. The experiment was repeated twice and data represents average of two experiments. AB+A and AB+B represent Δ*cnaA* Δ*cnaB* + *cnaA* and Δ*cnaA* Δ*cnaB* + *cnaB* strains, respectively. (B). 10^4 conidia from each calcineurin mutant were inoculated into 500 μl GMM broth on coverslips for a period of 18 h at 37°C and observed by microscopy. Highly branched hyphae in the Δ*cnaA* and the Δ*cnaB* strain with irregular septa can be seen. Delayed growth and swollen hyphae with irregularly formed septa can be observed in the Δ*cnaA* Δ*cnaB* strain. Scale bar, 20 μm. (C). Scanning electron micrographs of the wild-type strain and calcineurin mutants taken after a 48 h growth period. Note that while the wild type shows an evenly distributed hyphal mat, the Δ*cnaA* strain shows stunted hyphae with "club-like" shape. The Δ*cnaB* and the Δ*cnaA* Δ*cnaB* strains show compact colony morphology similar to the Δ*cnaA* strain, but have extensive extracellular fibrillar material forming a web-like network between the hyphae indicated by white arrows. Scale bars are indicated in the micrographs.
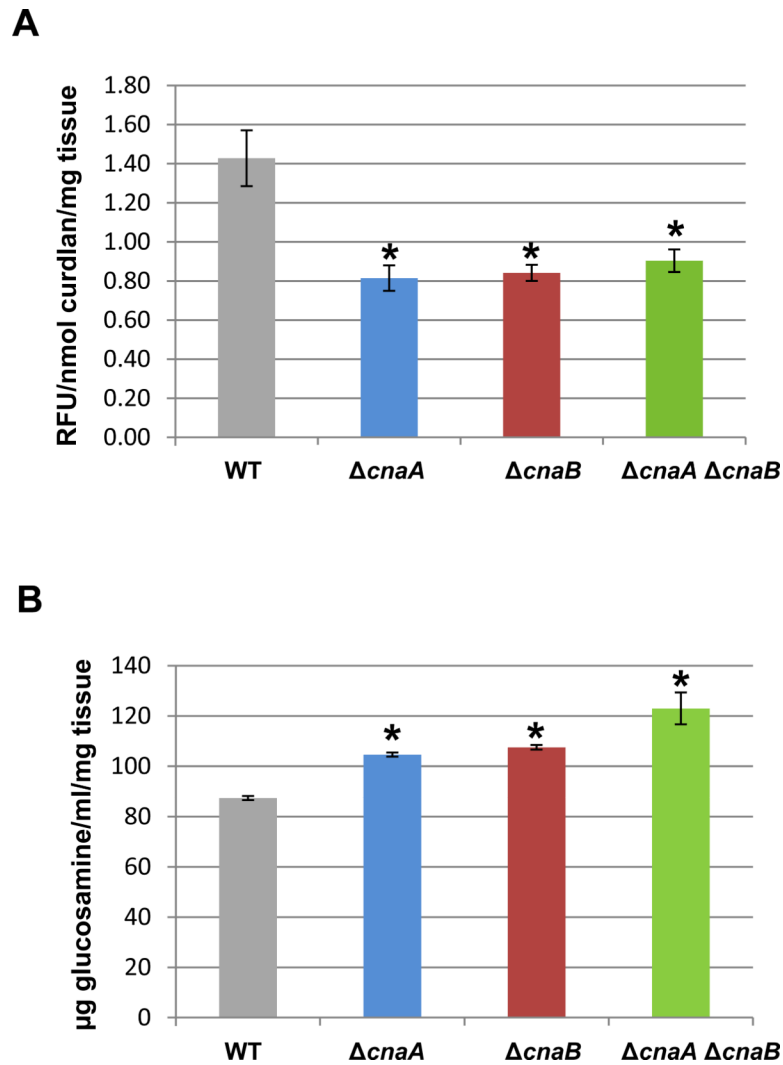
Figure 3.
Thickened cell wall and aberrant septa in the calcineurin mutants. The wild type and the calcineurin mutants were grown in GMM broth for a period of 48 h at 37°C and processed for transmission electron microscopy as mentioned in experimental procedures. Arrowheads indicate the irregular septa and dotted arrows indicate the thickening of the cell walls and the extracellular fibrous material. Magnification for panels A, D, E, G, H, J is 12,000X, for panels M and K it is 5000X, for panels B and N it is 30,000X and for panels C, F, I, L and O it is 50,000X.
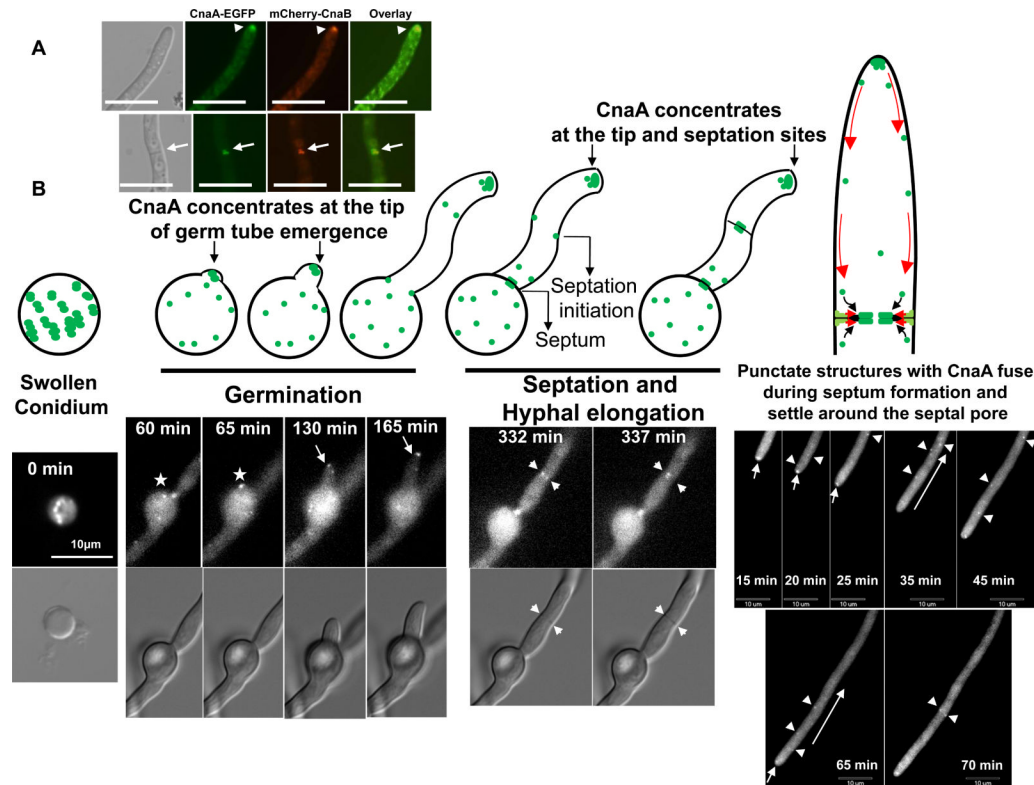
Figure 4.
(A). Calcofluor white staining of the wild-type and calcineurin mutant strains. A total of 1×10^4 conidia of the wild-type and the calcineurin mutant strains were inoculated onto coverslips immersed in GMM medium and grown for 24 h at 37°C. The coverslips were rinsed in sterile water, and inverted onto a 200 μl drop of calcofluor white staining solution for 5 minutes at room temperature. Coverslips were then rinsed twice for 10 minutes in sterile water and observed under fluorescent microscope. Scale bar, 10 μm. (B). For dual staining with calcofluor white and propidium iodide to observe septa and nuclei, first nuclear staining was performed by fixing the hyphae in 8% formaldehyde and staining with propidium iodide solution (12.5 μg/ml) in 50 mM PIPES (pH 6.7) for 5 min and then calcofluor white staining for 5 minutes at room temperature and observed under the fluorescence microscope. Scale bar, 10 μm. (C) Staining of cell wall β-glucan with aniline blue was performed on cultures grown on coverslips by inverting them onto a 200 μl drop of aniline blue (0.1 mg/ml) staining solution for 5 min at room temperature. Stained mycelia were directly observed by fluorescence microscopy. Note the absence of aniline blue staining of the septa in the Δ*cnaA* Δ*cnaB* strain. Arrows indicate septa. Scale bar, 10 μm. (D) Hyphal growth defect was quantified by measuring the apical, subapical and basal hyphal compartments in the single (Δ*cnaA* and Δ*cnaB*) and double (Δ*cnaA* Δ*cnaB*) mutants after growth for a period of 24 and 48 hours, respectively. Approximately 100 hyphal compartments were measured in each strain and the data depicts average lengths of the various compartments

A

B

Figure 5.
(A). β-1,3-glucan content was quantified using the aniline blue assay with curdlan, a β-1,3-glucan analog, as the standard. Values are expressed as relative fluorescence units per mg of mycelial tissue. The experiment was repeated three times and the results shown are mean ± standard error of three technical replicates. Asterisk indicates significance and $p < 0.03$ in comparison to the wild-type strain. (B) Quantification of chitin was performed and reported as glucosamine equivalents (μg/ml). The experiment was repeated three times and the results shown are the average of three technical replicates and error bars are standard errors. Asterisk indicates significance and $p < 0.006$ in comparison to the wild-type.
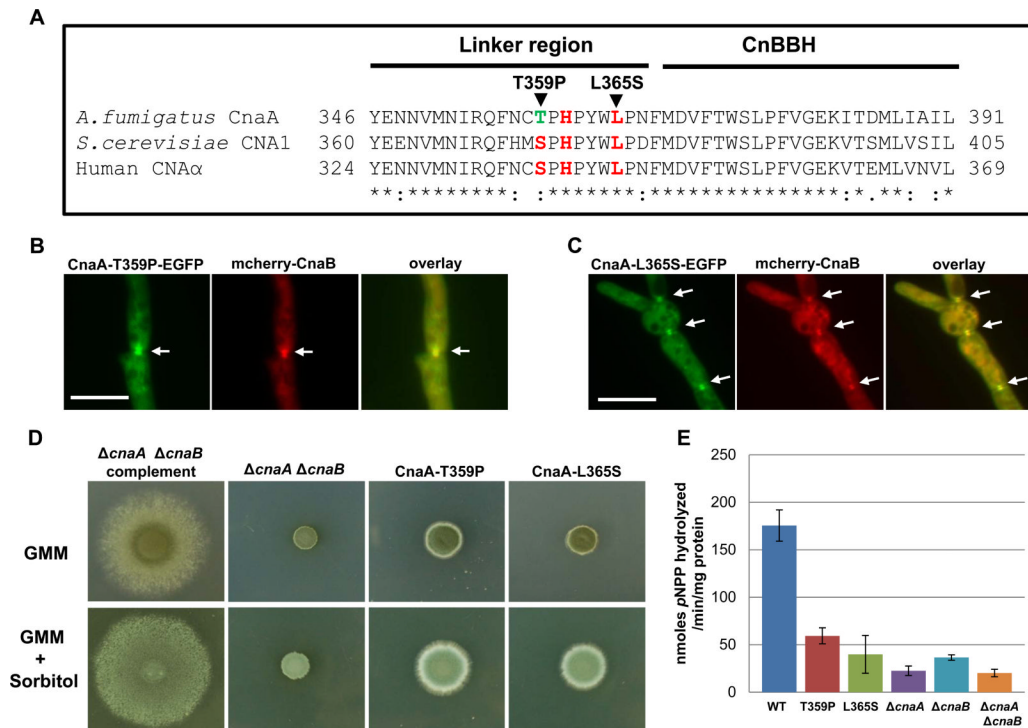
Figure 6.
(A). Co-localization of the CnaA and CnaB at the hyphal septum. The strain expressing CnaA-EGFP and mcherry-CnaB fusion proteins was visualized by fluorescence microscopy. Both CnaA and CnaB co-localized in dot-like structures (indicated by white arrowheads) and also at the center of the hyphal septum (indicated by white arrows). Scale bar, 10 μm.
(B). Dynamic distribution of CnaA-EGFP during germination, septation and hyphal elongation. Time-lapse series show *de novo* germination, septum formation and hyphal growth. Swollen conidia show CnaA-EGFP in dot-like vesicular structures (0 min). The site of germ tube emergence is indicated by an asterisk (60 and 65 min) and the arrows point to the movement of CnaA-EGFP in dot-like structures at the tip of the germ tube (130 and 165 min). During septation (332 and 337 min), the arrows point to the punctate structures on either side of the newly forming septum which then move towards the center of the septum and position on either side of the septum. The formation of septa can be clearly seen in the corresponding DIC images (indicated by small arrows). During hyphal extension the punctate structures seem to move retrograde from the tip towards the points of septation as indicated by arrowheads. Arrows indicate an initial tip gradient observed. Scale bar, 10 μm.
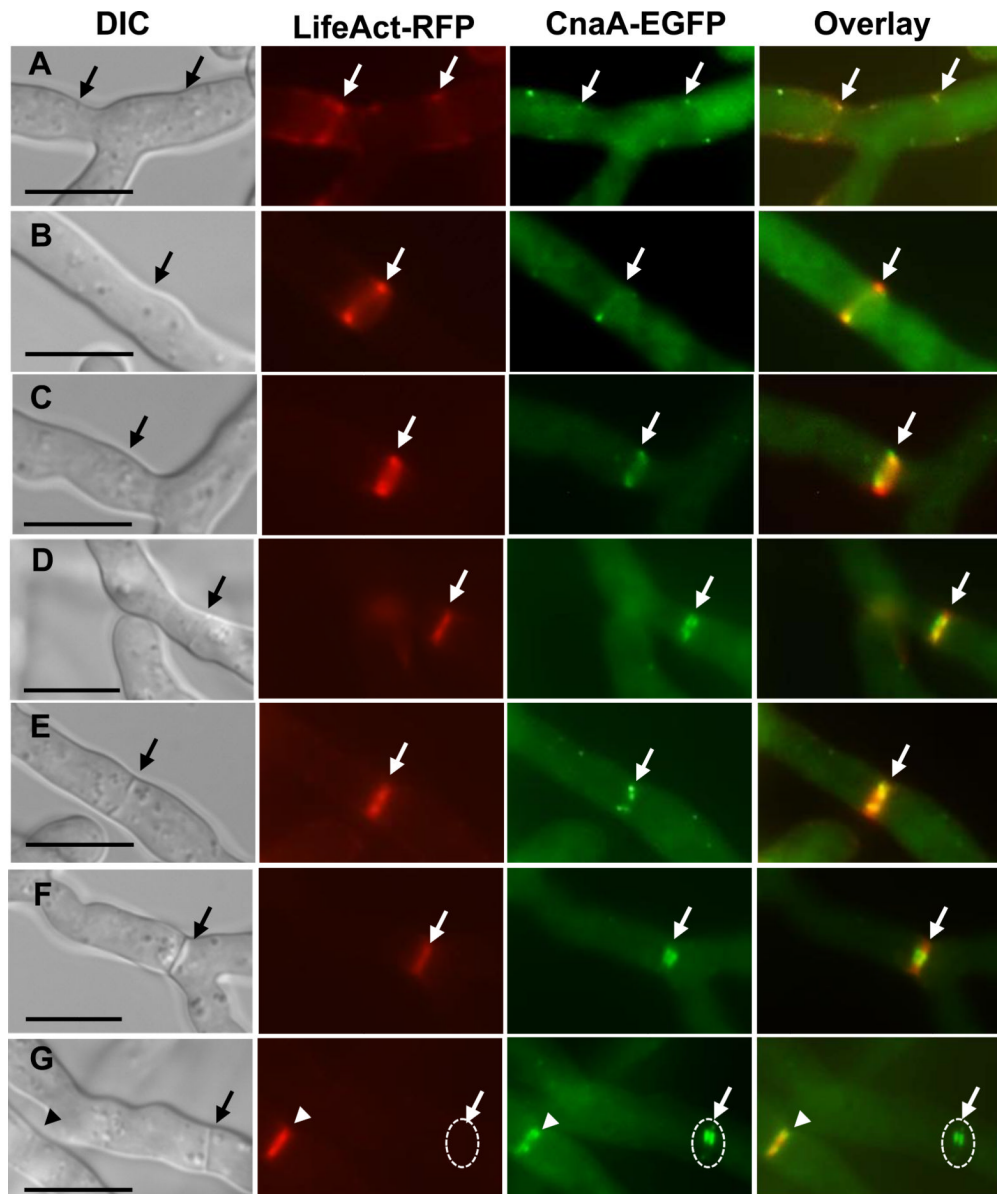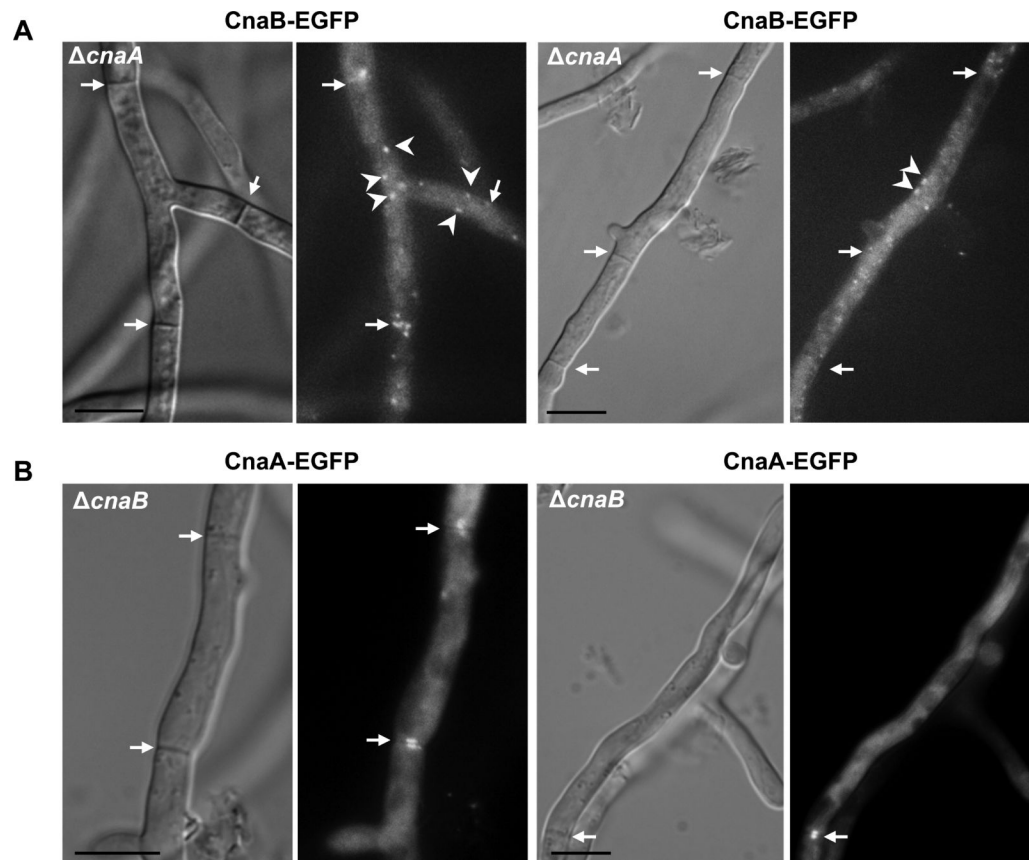
Figure 7.
Co-localization of CnaA-EGFP and actin at points of septation. The strain expressing CnaA-EGFP and Lifeact-RFP was visualized by fluorescence microscopy. Both CnaA and actin co-localized at the edges of contractile ring early in the septation process (panels A, B and C; indicated by arrows) and then as the septum formation occurred (Panels D, E, and F; indicated by arrows) CnaA-EGFP localized to the either sides at the center of the newly forming septum. After the completion of septum formation, actin ring constriction disappeared (Panel G; indicated by dashed circle), but CnaA-EGFP remained at the center of the septum (Panel G; indicated by white arrow pointing to a dashed circle). White arrowhead in panel G shows new point of septation. Scale bar, 10 μm.
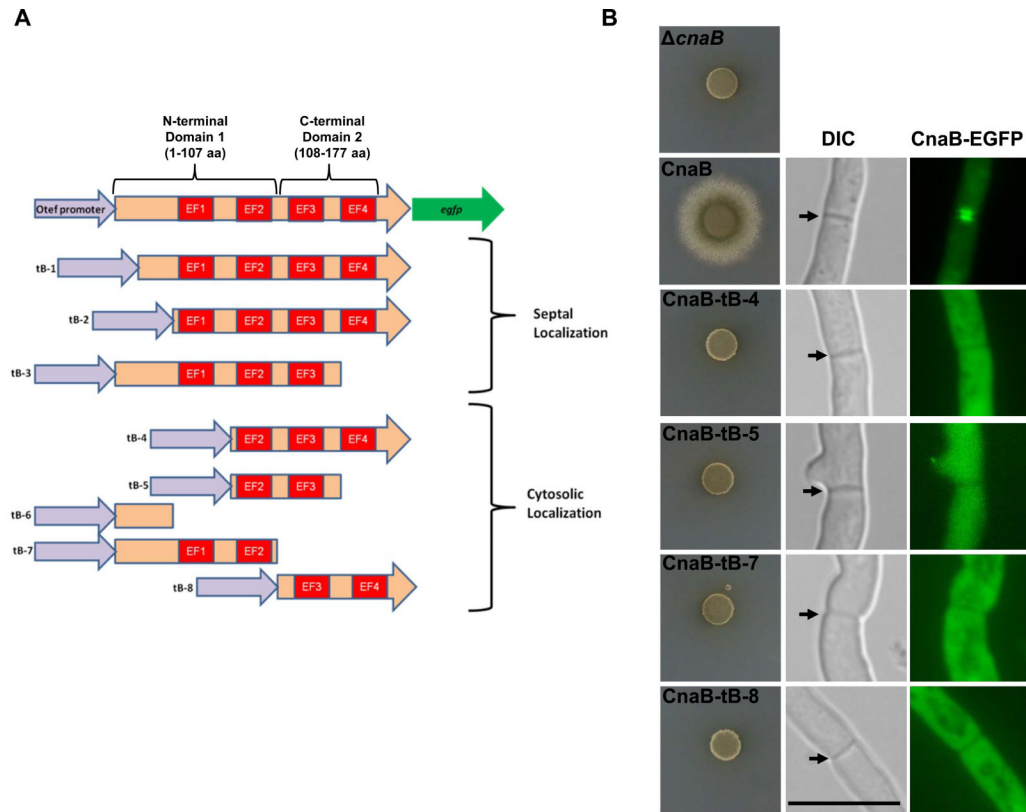
Figure 8.
Localization and activity of the calcineurin complex at the hyphal septum is required for proper hyphal growth. (A) Clustal alignment of the linker region between the catalytic domain and the CnaB-binding helix of CnaA. Residues in red represent the conserved active site residues. (B-C) Expression of the catalytic null mutated CnaAs (CnaA-T359P and CnaA-L365S) along with mcherry-CnaB in the Δ*cnaA* Δ*cnaB* strain showed the localization of the calcineurin complex at the hyphal septum (indicated by arrows). Scale bar, 10 μm. (D) Catalytic null mutations in CnaA do not complement hyphal growth. Radial growth of the indicated strains was monitored over a period of 3 days at 37°C on GMM agar medium or GMM supplemented with 1.2 M sorbitol. A total of 1×10^4 conidia were spotted for each strain. Note that both the T359P and L365S mutations did not restore hyphal growth (upper panel) and were only partially remediated in presence of sorbitol (lower panel). (E) Calcineurin phosphatase activity in the various strains was determined after a 48 h growth period using *p*-nitrophenyl phosphate as a substrate. The experiment was repeated two times and the results shown are mean ± standard error of six technical replicates. Note the drastic reduction in the catalytic null mutants and the calcineurin deletions strains.
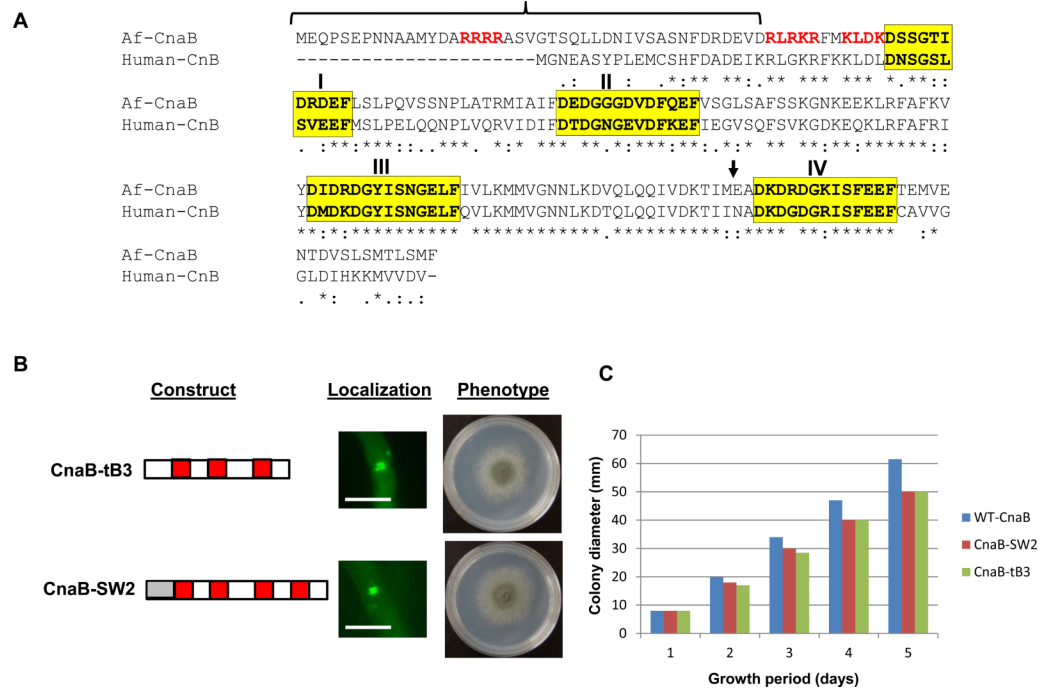
Figure 9.
CnaB does not localize to the septa in the absence of CnaA. (A). Expression of CnaB-EGFP fusion protein in the *cnaA* deletion background shows the presence of CnaB-EGFP in dot-like vesicular structures (indicated by arrowheads). These do not localize at the hyphal septa, indicating the requirement of CnaA for the localization of CnaB at the hyphal septum. Arrows indicate hyphal septa. Scale bar, 10 μm. (B) CnaB-independent localization of CnaA at the hyphal septum. Expression of CnaA-EGFP fusion protein in the *cnaB* deletion background does not affect the localization of CnaA at the hyphal septum. Arrows indicate the septal localization of cnaA-EGFP at the hyphal septa. Scale bar, 10 μm.
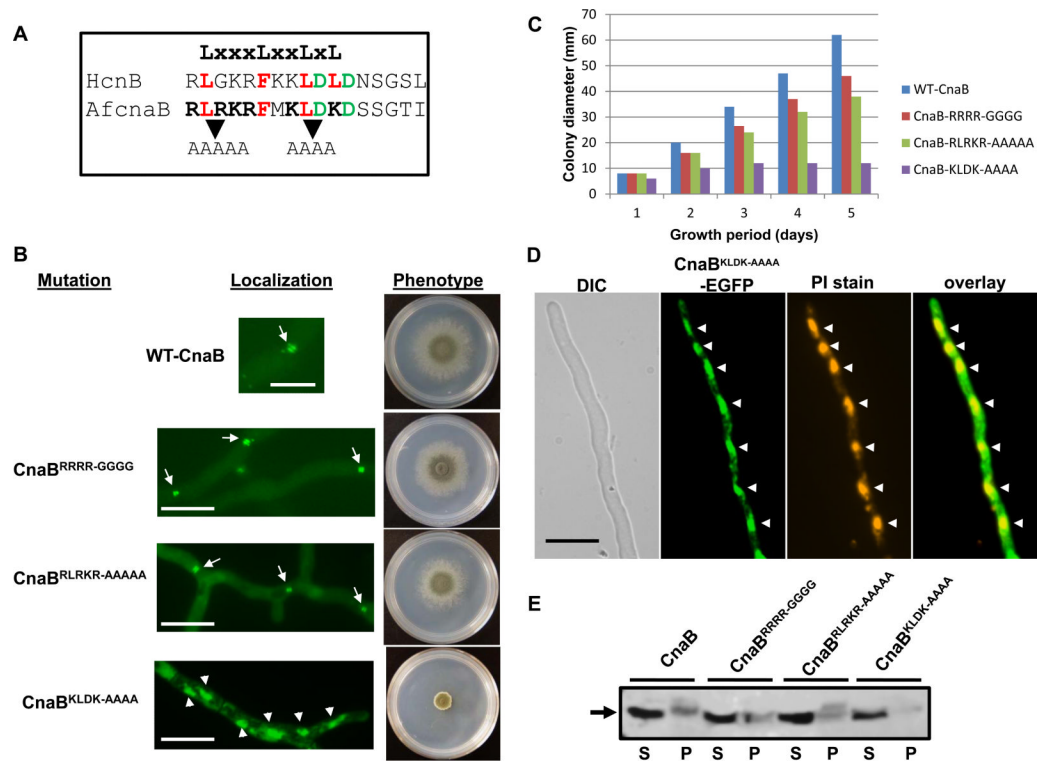
Figure 10.
Schematic model of domain organization in CnaB. (A) Scheme depicts CnaB truncation constructs (tB-1~tB-8) made in the four Ca^{2+}- binding motifs (labeled in red) and individually expressed as EGFP fusions under the control of the *otef* promoter in *A. fumigatus*. The truncations are grouped based on the localization pattern observed by fluorescence microscopy. Domain 1 is the N-terminal portion that includes the first 2 EF hand motifs and domain 2 is the C-terminal portion that includes the 3rd and 4th EF hand motif. (B). Complementation and localization analysis of the truncated forms of CnaB in the Δ*cnaB* strain. Conidia from strains expressing full length and truncated forms of CnaB-EGFP under the control of *cnaB* native promoter were spotted (1×10^4 conidia) on GMM agar medium and monitored for growth recovery for a period of 3 days at 37°C. Note that all the CnaB-truncations did not support hyphal growth. Fluorescence microscopy indicated complete cytosolic localization of the truncated CnaB fragments. Scale bar, 10 μm.

A

```
Af-CnaB      MEQPSEPNNAAMYDARRRRASVGTSQLLDNIVSASNFDRDEVDRLRKRFMKLDKDSSGTI
Human-CnB    --------------------MGNEASYPLEMCSHFDADEIKRLGKRFKKLDLDNSGSL
                                .:   .*:** **:.** *** *** *.**::
                 I                       II
Af-CnaB      DRDEFLSLPQVSSNPLATRMIAIFDEDGGGDVDFQEFVSGLSAFSSKGNKEEKLRFAFKV
Human-CnB    SVEEFMSLPELQQNPLVQRVIDIFDTDGNGEVDFKEFIEGVSQFSVKGDKEQKLRFAFRI
             . :**:***::.***. *:* *** **.*:***:**:.*:* ** **:**:***:**::
                   III                         ↓              IV
Af-CnaB      YDIDRDGYISNGELFIVLKMMVGNNLKDVQLQQIVDKTIMEADKDRDGKISFEEFTEMVE
Human-CnB    YDMDKDGYISNGELFQVLKMMVGNNLKDTQLQQIVDKTIINADKDGDGRISFEEFCAVVG
             **:*:********** *********** .*********:::**** **:****** .*
Af-CnaB      NTDVSLSMTLSMF
Human-CnB    GLDIHKKMVVDV-
             . *:  .*.:.:
```

B

C

Figure 11.

(A) Clustal alignment of *A. fumigatus* CnaB with human CnB1. Conserved residues are indicated in asterisks. The residues in four Ca^{2+}- binding motifs are highlighted in yellow. The N-terminal region shown in bracket indicates the extended amino-terminal region in comparison to human CnB1. Residues in red represent basic amino acid residues. Bold arrow indicates the position of truncation of the 4th EF hand motif (B). Expression of a truncated form of CnaB (CnaB-tB3; made by truncation of the 4th EF hand motif), and a domain swapped construct of CnaB (CnaB-SW2) made by the replacement of the extended N-terminal region of *A. fumigatus* CnaB with the N-terminal region of human CnB1 (shown in grey box) as mentioned in experimental procedures. Each construct was expressed as an N-terminal *egfp* tag in the *cnaB* deletion background. The transformed strains were verified for localization of the fusion constructs by fluorescence microscopy. Note that both CnaB-tB3-EGFP and the CnaB-SW2-EGFP fusion proteins localize at the hyphal septum. Scale bar, 10 μm. Hyphal growth recovery in the two strains was observed by inoculating a total of 1×10^4 conidia GMM agar medium and incubating at 37°C for 3 days. (C). Measurement of colony diameter of the strains expressing WT-CnaB, CnaB-SW2 and CnaB-T3 over a period of 5 days. For radial growth quantification the strains were grown on GMM agar medium in triplicate and values are depicted as average colony diameter.

Figure 12.

(A). Alignment of the predicted nuclear exit signal sequence (NES) at the N-terminus of human CnB1 and *A. fumigatus* CnaB is shown along with the NES consensus motif. Conserved residues in the LxxxLxxLxL motif are shown in red and other favored acidic residues are in green. Mutations in the RLRKR and KLDK motifs are indicated (B). Expression of mutated constructs of N-terminal basic motifs (15-ARRRA-20 to 15-AGGGGA-20, 44-RLRKR-48 to 44-AAAAA-48 and 51-KLDK-54 to 51-AAAA-54) in *A. fumigatus* CnaB by tagging with *egfp*. Note that while the control WT-CnaB, CnaB$^{RRRR-GGGG}$ and CnaB$^{RLRKR-AAAAA}$ expressing strains showed localization at the septa (indicated by arrows), the CnaB$^{KLDK-AAAA}$ strain showed nuclear localization (indicated by arrowheads). Hyphal growth recovery in the strains was observed by inoculating a total of 1×10^4 conidia GMM agar medium and incubating at 37°C for 3 days. WT-CnaB (blue bar), CnaB-SW2 (red bar), CnaB-tB3 (green bar). (C). Measurement of colony diameter of the strains expressing WT-CnaB (blue bar), CnaB$^{RRRR-GGGG}$(red bar), CnaB$^{RLRKR-AAAAA}$ (green bar) and the CnaB$^{KLDK-AAAA}$ (purple bar) strains over a period of 5 days. For radial growth quantification the strains were grown on GMM agar medium in triplicate and values are depicted as average colony diameter. (D). Nuclear staining of the strain expressing CnaB$^{KLDK-AAAA}$ tagged to *egfp*. Localization of the CnaB$^{KLDK-AAAA}$ in the nucleus was confirmed by propidium iodide staining of the nuclei. Arrowheads indicate the nuclei. Scale bar 10 μm. (E). Detection of the expression of mutated CnaB-EGFP fusion proteins. Total proteins (~50 μg) extracted from the strains cultured for 24 h were subjected to 12.5% SDS-PAGE and Western analysis using anti-GFP rabbit polyclonal primary antibody and peroxidase labeled anti-rabbit IgG secondary antibody. Detection was performed using the SuperSignal West Pico chemiluminescent substrate. S and P indicate supernate and pellet fractions, respectively.